Preparation and photophysical characterisation of pH sensitive sol-gel thin films doped with curcumin

Šiprak, Marija

Master's thesis / Diplomski rad

2022

Degree Grantor / Ustanova koja je dodijelila akademski / stručni stupanj: **University of Zagreb, Faculty of Chemical Engineering and Technology / Sveučilište u Zagrebu, Fakultet kemijskog inženjerstva i tehnologije**

Permanent link / Trajna poveznica: https://urn.nsk.hr/urn:nbn:hr:149:033117

Rights / Prava: In copyright/Zaštićeno autorskim pravom.

Download date / Datum preuzimanja: **2024-07-23**

FKITMCMXIX

Repository / Repozitorij:

Repository of Faculty of Chemical Engineering and Technology University of Zagreb

zir.nsk.hr

dabar
DIGITALNI AKADEMSKI ARHIVI I REPOZITORIJI

UNIVERSITY OF ZAGREB

FACULTY OF CHEMICAL ENGINEERING AND TECHNOLOGY

UNIVERSITY OF SPLIT

FACULTY OF CHEMISTRY AND TECHNOLOGY

GRADUATE UNIVERSITY STUDY PROGRAM

Marija Šiprak

MASTER THESIS

Zagreb, September 2022

UNIVERSITY OF ZAGREB

FACULTY OF CHEMICAL ENGINEERING AND TECHNOLOGY

UNIVERSITY OF SPLIT

FACULTY OF CHEMISTRY AND TECHNOLOGY

GRADUATE UNIVERSITY STUDY PROGRAM

Marija Šiprak

PREPARATION AND PHOTOPHYSICAL CHARACTERIZATION OF PH SENSITIVE SOL-GEL THIN FILMS DOPED WITH CURCUMIN

MASTER THESIS

Mentor: Prof. Ivana Steinberg, PhD

Members of the exam committee:
Prof. Ivana Steinberg, PhD
Assoc. prof. Svjetlana Krištafor, PhD
Prof. Ante Jukić, PhD

Zagreb, September 2022

ACKNOWLEDGEMENTS

SAŽETAK

Zbog svojih poželjnih kvaliteta, kao što su jednostavnost, prenosivost, jednokratnost i pristupačnost, optički kemijski senzori su u središtu intenzivnog proučavanja i razvoja, uključujući korištenje mikrofluidnih uređaja i takozvanih tehnologija laboratorija na čipu. Zbog svoje kompatibilnosti, cjenovne pristupačnosti, lakoće korištenja i obilja, papir se, uz staklo, koristi kao materijal za supstrat, a papirna mikrofluidika se uglavnom kombinira s kolorimetrijskim očitanjima. Nadalje, uporaba prirodnih „zelenih" boja kao pH osjetljivih bojila konstantno raste zbog ekoloških razloga, a među njima se ističe kurkumin, koji je privukao veliko zanimanje. Različita farmakološka djelovanja kurkumina dokazana su znanstvenim studijama, utvrđujući njegovu sposobnost za kemoprevenciju, kao i moguće terapeutsko djelovanje protiv raznih kroničnih bolesti. Nadalje, kurkumin ima jarko žutu boju u kiselim i neutralnim uvjetima, koja se pretvara u smeđe-narančastu kada je izložen bazičnom pH što ga čini obećavajućim alatom za trenutnu detekciju analita golim okom, bez upotrebe sofisticiranih instrumenata. U ovoj studiji, optički senzori za brzo očitavanje pripremljeni su korištenjem kurkumina kao pH bojila, imobiliziranog sol-gelom metodom i položenog na dvije različite vrste podloga, staklo i papir. Izrađeni senzorski materijali temeljeni na kurkuminu karakterizirani su primjenom UV-Vis apsorpcijske i reflektancijske spektroskopije, a kolorimetrijska detekcija ispitana je u rasponu pH vrijednosti od 4 do 13. Zaključeno je da su papirnati senzori na bazi kurkumina postigli bolje rezultate od staklenih senzora, što je dovelo do dodatnog testiranja njihove stabilnosti i reverzibilnosti.

KLJUČNE RIJEČI: *optički kemijski senzori, papirna mikrofluidika, prirodna "zelena" bojila, pH osjetljiva bojila, kurkumin*

SUMMARY

Due to its desirable qualities, such as simplicity, portability, disposability and affordability, optical chemical sensors have been the focus of intensive study and development, including employment of microfluidic devices and lab-on-a-chip technologies. Due to its compatibility, affordability, user-friendliness and abundance, paper, alongside glass, has been used as a substrate material, and paper-based microfluidics have been mostly combined with colorimetric readouts. Furthermore, employment of natural "green" dyes as pH-sensing colorants is rising due to environmental reasons, and curcumin is therefore attracting major interest. Curcumin's various pharmacological actions have been proven by different scientific studies, establishing its ability to operate as a chemo-preventive, as well as potential therapeutic agent against a variety of chronic diseases. Furthermore, curcumin has a bright yellow color in acidic and neutral conditions that turn into a brownish-orange color on exposure to a basic pH solution. This makes it a promising tool for instantaneous detection of analyte with the naked eye, without the need to use the sophisticated instruments. In this study, optical sensors for quick sensing were created utilizing curcumin as pH indicator, immobilized by sol-gel method and deposited on two different types of substrates, glass and paper. Curcumin-based sensors were characterized by UV-Vis absorption and reflectance spectroscopy as well as colorimetry, on exposure to solutions of pH ranging from 4 to 13. In conclusion, curcumin-based paper sensors achieved better results than curcumin-based glass thin films, which lead to their further characterization in terms of stability and reversibility of response.

TABLE OF CONTENTS

1. INTRODUCTION

In the past few decades, optical chemical and biochemical sensors have become the subject of extensive research and development due to their desirable properties like simplicity, portability, affordability and disposability [1,2]. Furthermore, they showed exceptionally good results in detecting contaminants including metals, pathogenic microorganisms, antibiotics, residues and pesticides, and therefore, have been used in industrial, environmental, and biomedical monitoring, (*e.g.* in food packaging, for diagnosis of some diseases, and for examining nutrients in soil) [2-4]. When it comes to the working principle of optical sensors, their response is based on the change of optical properties of the chemical reagent upon interaction with the analyte of interest in the solution. The most commonly measured optical properties are absorption, fluorescence intensity, and decay time, while reflectance, refractive index, light scattering and light polarization can also be measured, but are less employed [5,6].

Most optical pH sensors reported the use of colorimetric and fluorescent indicator dyes so that the change in the optical property of an analyte-sensitive dye is used to monitor analyte concentration [5]. Until recently, only synthetic dye colorants were used, *e.g.* bromophenol blue, bromocresol green and phenol red. They were shown to be toxic for the environment and threatening to human health, so researchers decided to try using natural colorings instead [3,4,6]. One of the natural dyes that received a high interest in recent years is curcumin, thanks to its anti-inflammatory, anti-bacterial, anti-cancerous, antimicrobial and antifungal properties [2,4]. Furthermore, due to its beneficial medicinal properties, as well as low toxicity and outstanding photostability, curcumin became a highly potential compound for sensing applications, and has already been used in food industry for visually detecting the spoilage of shrimps, as well as in healthcare for magnetic resonance imaging (MRI) [2,4,7].

One of the most popular techniques for indicator dye immobilization into the solid support is sol-gel technique, due to its easy fabrication procedure, flexibility of process design, and production of high-performance pH sensor material with long-term stability [1,6]. The basic principle of mentioned technique is permanently anchoring dye molecules within a porous silica matrix through which analytes and protons can penetrate and interact with the trapped

dye [6]. In recent decades, there has been an increased interest for optical pH sensors based on sol-gel materials, but the main problem with this type of sensors is relatively narrow pH range, especially when natural dyes are used as pH-sensing colorants [3,6].

Hence, examination of pH sensitivity of bioactive molecules from natural resources, especially study of their immobilization in different matrices and its effects on sensing response, present an attractive research field. In this work, a development of an analytical platform for a rapid naked-eye colorimetric detection of pH in the range 4 – 13 has been presented. Sensing materials were designed and fabricated using curcumin immobilized by sol-gel method, on two different substrates, glass and paper. Sensing materials were exposed to buffer solutions and subsequently characterized by UV-Vis absorption and/or reflectance spectroscopy. In conclusion, curcumin-based paper sensors achieved better results than curcumin-based glass thin films, which lead to their further characterization in terms of stability and reversibility of response.

2. GENERAL PART

2.1. OPTICAL CHEMICAL SENSOR

Optical chemical sensors have replaced classical solutions for chemical sensing which are complex and expensive, and have been used for biomedical and industrial application due to their real time and continuous monitoring [5]. Furthermore, miniaturization of sensing techniques provided lower costs, faster response time and greater accessibility which allowed lower-cost markets like residential sensing of toxic chemicals, detection of seafood freshness, breath alcohol analysis, to employ optical chemical sensors [5-7]. Every optical chemical sensor consists of four main components [5]:

- sample (analyte),
- transduction platform (sensing platform transduction),
- signal processing element (electronics), and
- optical signal measurement (analyte concentration).

The working principle of a chemical sensor is based on employing optical transduction techniques, meaning that upon interaction of reagent, which is usually an analyte-sensitive dye, and the analyte of interest, reagent changes its optical properties which are utilized to monitor analyte concentration [1,5]. The most commonly measured optical properties include absorption, fluorescence, intensity and decay time, while reflectance, refractive index and light scattering/polarization can also be measured, but are generally far less employed [1,3,5].

2.1.1. Optical pH Sensor

In the past few decades, there has been an increasing interest in optical sensors based on the use of immobilized pH indicators since pH is one of the key target parameters in a broad range of applications [5,6]. Optical pH sensors, also called optodes, consist of two main parts: 1) an organic carrier which is a proton-permeable solid matrix, and 2) an acid-base pH indicator which can be adsorbed on the surface of a matrix, chemically immobilized or physically entrapped in polymeric matrices, *e.g.* by sol-gel method [5,7,8].

The working principle of optodes is based on exploitation of pH indicator dyes, typically weak organic acids or bases, with distinct optical properties related to their protonated (acidic) and deprotonated (basic) forms [5]. With the change of concentration of hydronium ions, the absorption (color) of these dyes changes as a function of the pH of the environment [5-8]. Because sensors don't measure the pH of the solution directly, but measure the concentration of the acid or base form of an indicator dye molecule instead, the final measurement of pH depends on the pK_a (dissociation constant) of the dye, and therefore, provides a smaller dynamic range [5,6]. Even though the narrow pH range was initially a barrier to broader applications of optical pH sensors, researchers successfully resolved the problem by using indicators with two pK_a values or a group of similar dyes with different pK_a values [5,6,8].

When building an optical pH sensor, two criteria need to be considered: first one is selection of a suitable materials and detection methods, and second is sensor characterization which includes determination of [5]:
- real time response,
- reversibility,
- reproducibility,
- sensitivity,
- shelf life,
- operational stability,
- photostability, and
- degree of leaching.

Furthermore, sensor application dictates its characteristics, which are determined by properties of a pH sensitive dye and pH sensing matrix [5,6]. When it comes to desired properties of a pH sensitive dye, besides already mentioned appropriate pK_a value, it also needs to have high excitation coefficient, emission band in the visible region, good photostability, and it needs to be chemically and thermally stable. pH sensing matrix should also be chemically and thermally stable, as well as mechanically stable, hydrophilic (to facilitate proton diffusion), compatible with deposition techniques, and most importantly low-costly [5,6,9].

2.2. SENSING SUBSTRATES

Microfluidic devices and lab-on-a-chip technology have been recognized as a promising platform for ultrasensitive bioanalytical devices, point-of-care (POC) diagnostics and health monitoring systems, and have gained widespread recognition with applications in areas like investigation of cell biology and tissue engineering, mixing and separation of bio-species, drug discovery, biohazard detection, as well as automating synthetic biology to create micro-organism and DNA foundries [10,11]. Materials like polydimethylsiloxane (PDMS), polymethyl methacrylate (PMMA), chromatography paper, glass, silicon, and others can be used to create such versatile microfluidic devices [11]. In this research glass slides and filter paper have been used as pH sensing substrates, and therefore their properties, including advantages and disadvantages will be further discussed in the next paragraphs.

2.2.1. Glass

Microfluidic devices must have exceptional optical transparency, mechanical, chemical, and thermal stability, as well as simple design and fabrication, in order to attain higher performance, and due to its exceptional optical, mechanical, thermal, electrical, and chemical properties in comparison to other materials (e.g., silicon and PDMS), glass has become an appealing and perfect medium for the production of microfluidic devices [10,11]. Glass stands out among other materials because of its high transparency, temperature resistance, and compatibility with other solvents [11]. Furthermore, high chemical stability, pressure resistance, hydrophilicity, and adaptability to a variety of surface biofunctionalization processes are just a few of the other benefits of glass, but expensive manufacturing costs of Si-glass microchips have limited their use, especially with the development of paper-based microfluidics. [10,12].

2.2.2. Paper

Just like traditional microfluidic devices made from silicone, glass or polymers (*e.g.* PDMS or PMMA), paper-based microfluidic devices are portable, process small volumes of fluids, and can perform multiplexed assays, but they have several advantages over conventional microfluidic devices including [13-15]:

- easy operation and fabrication,
- lower cost,
- easier disposal, and
- the ability to operate without pumps or other supporting equipment (power-free).

Furthermore, paper is well suited for biomolecule immobilization because of high physical absorption, bio-affinity, and bioactive ink entrapment, and there is no need for further functionalization of the substrate, while in the case of glass, it is frequently necessary to modify substrate in order to achieve bio-functionality [10]. The two forms of cellulose-based paper that are most frequently utilized for the creation of µPADs (paper-based analytical devices) are filter paper and chromatography paper, while colorimetric readouts are the most common detection method used in PADs because the white background of the paper substrate provides high contrast to the colorimetric signals, offering a good signal-to-noise ratio for the detection, enabling straightforward interpretation of the results [13,14]. On the other hand, since paper is not optically transparent, it's not well suited for absorbance spectroscopy, while other disadvantages of paper-based devices include short shelf life of reagents stored on the devices, the coffee ring effect where solutes tend to aggregate around the outer edges test zones as the solutions dry out on paper, and lastly, any application of paper-based devices will contain indeterminate mistake due to the inherent unpredictability of paper [13].

2.3. IMMOBILIZATION TECHNIQUE

Besides selecting a proper sensing matrix and a proper indicator dye, the performance of the sensor is also significantly influenced by the way in which the sensor components are immobilized or bonded to the matrix, and therefore, if this bond is weak, it is intuitively clear that the sensor application will be limited [5,7]. There are two main types of bonding: physical, which includes adsorption as its simplest form, which is not recommended in optical sensors because stability is lost in the long run due to the inevitable leaching, so chemical bonding is the second and better alternative which allows physical trapping of an indicator dye in the polymer matrix, and one of the best examples of it is sol-gel method [7].

2.3.1. Sol-Gel

The sol-gel process is extremely simple, and is based on hydrolysis and polycondensation reactions of organometallic precursors to create inorganic networks which are transparent and allow the diffusion of analytes, but more importantly, in which indicators and other sensor components can be trapped during their formation, which makes them suitable for optical sensor applications [16-18]. Furthermore, sol-gels are ideal for use as sensor matrix supports because they are exceedingly inert and compatible with a wide range of chemicals agents, while the process can be carried out at room temperature and doesn't require high temperature heating for production of glass-like properties which allows temperature-sensitive organic molecules to be used as sensing transducers [16]. Other advantages of the sol-gel process include production of a wide range of novel functional materials with different morphologies, *e.g.* monoliths, films, fibers and powders, and lastly and most importantly, costs of production are low [16,18].

In general, sol-gel process includes two main steps [16,19]:
1. "Sol" formation, which is a stable dispersion of colloidal particles (amorphous or crystalline) or polymers in a solvent, in which van der Waals forces or hydrogen bond dominate, and
2. "Gel" formation, also called gelation step, in which a three-dimensional continuous network containing a liquid phase is formed, and in which covalent-type interactions dominate.

In gelation step, hydrolysis and condensation are two main reactions which are carried out, followed by aging, solvent extraction, and finally drying (Figure 1.) [16].
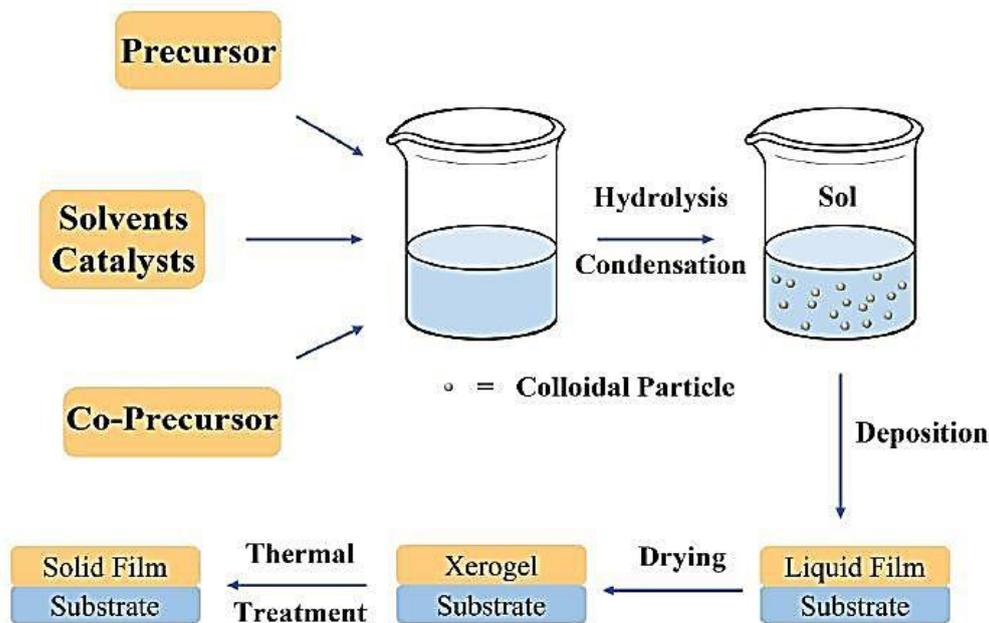
Figure 1. Diagram of the main steps in the sol-gel process [20].

In most cases, catalysts are added to facilitate hydrolysis, and when silicate derivates are used as starting material, hydrolysis can be carried out in two ways: addition of an acidic catalyst leads to acidic hydrolysis and production of monoliths, while basic hydrolysis is based on addition of a basic catalyst, leading to formation of nanostructures [16,19]. The rate of hydrolysis is firstly and mostly influenced by the strength and concentration of the acid or base catalyst, and then secondly by temperature and solvent [17,19]. One of the problems with sol-gel is that sometimes syneresis can occur, which involves deformation of the network and transport of liquid through the pores leading to spontaneous shrinkage of a gel during the aging of the gel, or during drying as the liquid evaporates [16,17].

2.3.1.1. Precursors

As already mentioned, sol-gel chemistry is based on reactions of organometallic compounds such as alkoxides, nitrates, or chlorides, under aqueous conditions with the aim of forming solid product, *e.g.* dense glass monolith, high surface area filter, metal oxide, nanoparticle or aerogel [16]. The class of precursors most widely used in sol-gel research are alkoxides, especially alkoxides of titanium and silicon derivates, because they readily react with water, and the most thoroughly studied metal alkoxides are tetraethoxysilane ($Si(OC_2H_5)_4$) and

tetramethoxysilane (Si(OCH$_3$)$_4$), which are abbreviated in the literature as TEOS and TMOS respectively (Figure 2.) [17,19].
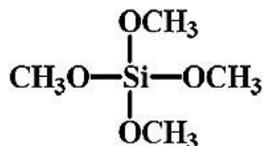
Tetramethyl orthosilicate (TMOS)   **Tetraethyl orthosilicate (TEOS)**
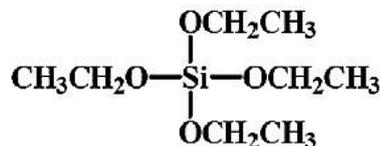
Figure 2. Structures of mesoporous silica precursors [19].

In recent years, an advancement was achieved by copolymerization of inorganic precursors with organic functional groups, resulting in inorganic/organic hybrid materials called Organically modified Silicates, or shortly OrmoSils [21]. Introduction of mentioned OrmoSil functional group allowed immobilization of reagent via covalent bonding, but it also improved chemical and physical properties of inorganic sol-gel materials, including better wettability, biocompatibility, varying degrees of lipophilicity, etc., and improved mechanical properties including better adhesion to the substrate, easier shaping and pattering and crack-free surface [21,22].

2.3.1.2. Design of Materials

When it comes to design of sol-gel materials, sensitivity to different parameters needs to be taken into account, including [16]:

- pH – all water-based systems are sensitive to pH,
- Solvent – has two key roles: keeping the dissolved nanoparticles so they don't precipitate out of the liquid, and helping nanoparticles connect with each other,
- Temperature – formation and the assembly of nanoparticles in a gel network is accelerated with temperature; at very low temperature, gelation is slow (can take weeks or months for gel to form); at very high temperature, lumps form and solid precipitates out of the liquid,

- Time – recommended to have a slow gel formation to produce a very uniform structure, resulting in a stronger gel; accelerating reactions can cause precipitates to form, or cause a gel to become cloudy or weak, or simply not form,

- Catalysts – accelerate chemical reaction, especially hydrolysis, but increases pH sensitivity because acids and bases accelerate chemical reactions by different mechanisms,

- Agitation – mixing of the sol during gelation should ensure uniform production of chemical reactions, including allowing all molecules to receive an adequate supply of chemicals needed.

In optical film production, sol-gel is highly employed because it provides tough, thin, inert and resistant films, produced from a single mixture of chemicals (one-pot synthesis) making it suitable method for high volume manufacturing [3,21]. Furthermore, versatility of sol-gel materials allows applications in wide range of fields, including energy, electronics, and environmental pollution, but it also allows the encapsulation of biological molecules such as proteins and enzymes, enabling its usage in biosensors for drug release, or tissue engineering [16].

2.4. DEPOSITION TECHNIQUE

As already mentioned, sol–gel technology is particularly suited for integrated chemical sensing solutions, as it allows for a one-pot synthesis of the functional sensing material while also being compatible with various deposition processes like spin-, dip-, and spray-coating [23]. In this research, spin coating was used as a deposition technique so it will be further explained in the next paragraph.

2.4.1. Spin Coating

Spin coating is the most commonly used deposition technique for the fabrication of thin films thanks to its simplicity, the relatively inexpensive equipment used, and the obtainable good results, providing uniform coatings of organic materials on flat surfaces [24-26]. Spin-coating method is based on centrifugal deposition and the whole process consists of few steps (Figure 3.) [24,26]:

i.   the hydrophilic substrate is fixed to a plate by an aspirator,

ii.   the coating solution is deposited on a substrate using a pipette, and

iii. the solution is spread uniformly across the whole surface of substrate by spinning the plate to high angular velocities (hundreds to thousands of rpm) to spin-off excess solution.

Figure 3. Different stages of spin coating [26].

During spinning, solvent contained in the coating solution starts to evaporate which leads to an increase in viscosity, and facilitated formation of the solid-like gel film, making the whole process quick, and suitable for sol-gel immobilization [24]. As a result, thin and uniform films are achieved, and their thickness can be controlled by the viscosity of the coating solution and the rotation speed [24-26].

When compared to other deposition techniques, like dip-coating, vapor-phase deposition, vacuum deposition, etc. main advantages of spin-coating technique include good reproducibility, easy integration with conventional lithography-based fabrication techniques, relative inexpensiveness, as well as already mentioned easy and quick deposition of thin

layers, but on the other hand, as the size of the substrate increases, high-speed spinning becomes more difficult, making it limited in scalability, and more than 90% of the coating material is flung off and disposed in the process leading to high material losses [24-26]. Furthermore, spin coating is not favorable for creating multilayer structures with more than two layers, or extremely thin films with thickness < 10nm [26].

2.5. OPTICAL DETECTION OF ANALYTE

The main goal of optical measurements is to collect the analytical information upon interaction between radiation and matter, and the most important type of radiation for sensors is electromagnetic radiation which makes spectroscopy the best method for optical detection of analyte [27,28]. Spectroscopy is focused on the production, determination, and identification of spectra that are formed by electromagnetic radiation interacting with samples, and therefore, provides information about the sample regarding its structure and molecular composition by employing simple, quick, highly precise and accurate methods, which are also relatively inexpensive compared to chromatography, electrophoresis or other analytical methods [28]. Because not all spectroscopic observations can be employed in sensors, only a subset of the spectroscopic wavelength range is important for sensor applications- the ultraviolet and visible (UV-Vis) spectral regions, as well as the infrared (IR) region, are the most essential parts of the electromagnetic spectrum for chemical sensors, making UV-Vis and IR spectroscopy the primary detection methods [27]. There are three main ways in which radiation can interact with an analytical sample [27,28]:

• Absorption,

• Reflectance and refraction, and

• Scattering (including fluorescence and phosphorescence).

In the next paragraph, main principles of absorption and reflectance will be further explained since they were used in this research, while basic principles of other spectroscopic techniques can be found in the literature [27,28].

2.5.1. Absorption

Absorption is based on measuring the intensity of light absorbed by an optically active analyte, or a corresponding indicator when electromagnetic radiation passes through a transparent medium [29]. The absorption of photon energy leads to a change in the energy states of the molecules in the sample; by absorbing a photon of UV-Vis light, electrons from the ground energy state are excited into short-lived excited states, in other words, an electron is promoted from the molecule's HOMO (Highest-energy Occupied Molecular Orbital) to the LUMO (Lowest-energy Unoccupied Molecular Orbital) [27-29]. The HOMO is often a conjugated functional group's π orbital, while the LUMO is commonly a conjugated functional group's π^* orbital, and the narrower the energy difference between HOMO and LUMO, the less energy is required, and the wavelength absorbed is longer [9]. The amount of energy required to excite an atom or molecule is unique to each species, hence it can be used to distinguish them, and therefore, these energy transitions are used to identify unknown substances in both absorption and emission spectroscopy [28].

Quantification od analyte is based on Lamber-Beer's law [28]:

$$(A)_\lambda = \left(\log \frac{I_0}{I_T}\right)_\lambda = \varepsilon \cdot l \cdot c \tag{1}$$

where c is concentration of the absorbent species (analyte or indicator); l is the length of the path that the electromagnetic radiation must travel through the medium; ε is proportionality constant called absorptivity or molar absorption coefficient which speaks of the probability of electronic transitions between the energy states of a molecule.

As the name implies, in UV-Vis absorption spectroscopy, absorption of light in ultraviolet (200 to 400nm) and visible range (400-750nm) is employed, so when a compound absorbs a specific wavelength or color from white light, the reflected wavelengths combine to give the compound a complimentary hue, and even though the exact cutoffs for these color ranges are subjective, most reference sources cite values that are comparable to those listed on Figure 4. [9,28].
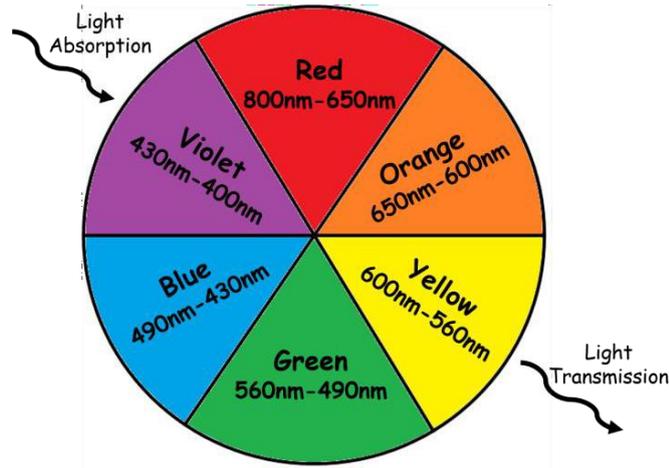
Figure 4. Light color wheel [30]

2.5.2. Reflectance

This technique is applied when it is necessary to perform measurements in light-tight media such as paper and textiles, mainly with the use of optical indicators [29]. Reflectance is based on measuring the intensity of the reflected beam (I_R) in relation to the incident bean (I_0) after reflection from the surface of the measured medium, and is defined as the ratio of these two intensities [31]:

$$R = \frac{I_R}{I_0} \tag{2}$$

The model set by Kubelka and Munk is the most often used to connect the relationship between radiation intensity and the concentration of optically active species, where the basic assumption is that the incident and reflected radiation is perfectly diffused, and the measurement principles of diffuse reflectance are analogous to the measurement of absorbance [32,33]. The K-M model defines reflectance as a function of light absorption and scattering caused by optically active substances (indicators) and particles in substrate materials (such as paper or textiles) [32]:

$$f(R)_\lambda = \left(\frac{(1-R)^2}{2R}\right)_\lambda = \frac{\varepsilon \cdot c}{s} \tag{3}$$

where c = concentration of the absorbent species (mainly indicator); ε = molar absorption coefficient (absorptivity); and S = light scattering coefficient. It should be emphasized that

the K-M model, like Lambert-Beer's law, is applicable only to monochromatic radiation, and in this way, the results obtained can be compared with absorbance measurements [31,33]. Furthermore, the absorption and scattering coefficients in the K-M model are constants which can be determined for each wavelength of incident radiation [33].

2.6. CURCUMIN

For pH monitoring colorimetric sensors are a common approach because they are simple to use, affordable, and may be utilized on-site, and in recent few decades, there has been an increased interest for employing natural plant resources as colorants [3]. In this study, bioactive compound curcumin from turmeric was used to construct biosensors for pH assessments so its theoretical background is presented in the following paragraphs.

Curcumin is a natural yellow pigment extracted from *Curcuma longa* L., also known as Indian curry spice Turmeric, and is made up of three main phenolic compounds, named curcuminoids (Figure 5.) [34]. Curcumin is known for its wide range of health-promoting and disease-preventing effects, such as suppression of carcinogenesis, anti-inflammatory activities, preventing expansion of tumor cells (*e.g.* skin, lunger, stomach, colon, and breast), as well as having antioxidant, antifungal, analgesic and neuroprotective properties [34-37]. Furthermore, it is a powerful metal chelating agent and an efficient radical scavenger, and it possesses excellent chromogenic properties, including large molar extinction coefficient, high fluorescence quantum yield and visible light excitation, as well as long-wavelength emission, low toxicity and outstanding photostability which make curcumin a great potential as a photosensitizer and a natural dye molecule [36,38].
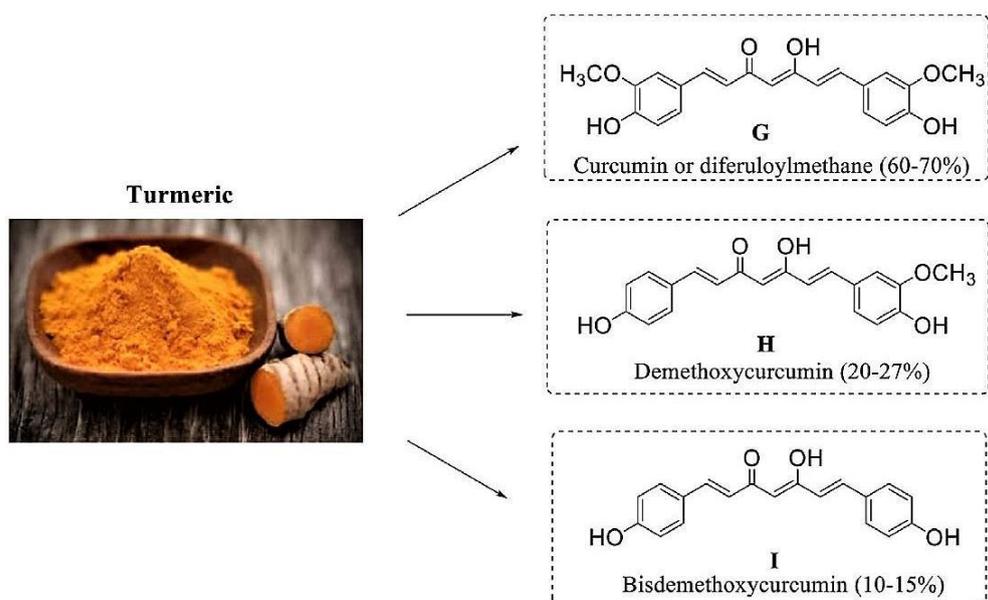
Figure 5. Phytochemicals of extract of *Curcuma longa* L. [34]

2.6.1. Physical and Chemical Properties

Curcumin is also known as diferuloylmethane, with chemical formula $C_{21}H_{20}O_6$, while its nomenclature according to International Union of Pure and Applied Chemistry (IUPAC) is ((1E,6E)-1,7-bis(4-hydroxy-3-methoxyphenyl)-1,6-heptadiene-3,5-dione) [34,37]. Curcumin is a symmetric molecule with two aromatic ring systems containing o-methoxy phenolic groups connected by a seven-carbon linker consisting of an α, β-unsaturated β-diketone moiety [37]. Furthermore, curcumin exhibits keto-enol tautomerism (Figure 6.) which means that it can exist in different types of conformers depending on the environment: solvent and pH, so in most non-polar and moderately polar solvents, as well as in alkaline pH, it exists in enol form which is also more stabilized than the keto form, while in polar solvents and acidic and neutral solutions, keto form is favorable [34,35,37].
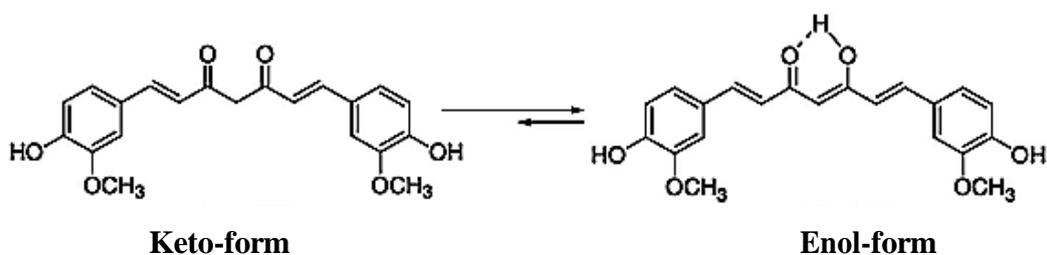
Figure 6. Keto-enol tautomerism of curcumin [39].

Curcumin is a weak Brönsted acid with three labile protons and three pK_a values that are defined by the following equilibrium reactions [34,37]:

- $H_3Cur \rightarrow H_2Cur^- + H^+$ $\rightarrow$ pK_{a1} (hydrogen from acetylacetone group)

- $H_2Cur^- \rightarrow HCur^{2-} + H^+$ $\rightarrow$ pK_{a2} (hydrogen from the phenol group)

- $HCur^{2-} \rightarrow Cur^{3-} + H^+$ $\rightarrow$ pK_{a3} (hydrogen from the phenol group).

Exact values of pK_a values and chemical structures of curcumin as it undergoes deprotonation are presented on Figure 7. The first pK_a is in the pH range of 7.5 to 8.5 where recognizable color change occurs, from yellow in an acidic media to red in a basic media, but increase in pH does not just cause color change, it also contributes to increased chemical reactivity and solubility of curcumin, making anionic curcumin more water soluble than in the neutral form [37]. Poor aqueous solubility of curcumin in neutral aqueous medium is a major problem in its bioavailability, but there are ways to increase it, *e.g.* by encapsulation in surfactant micelles [40], phospholipids [41], hydrogel [42], polymeric micelles [43], or by chemical alteration [44], complexation or interaction with macromolecules [45,46].
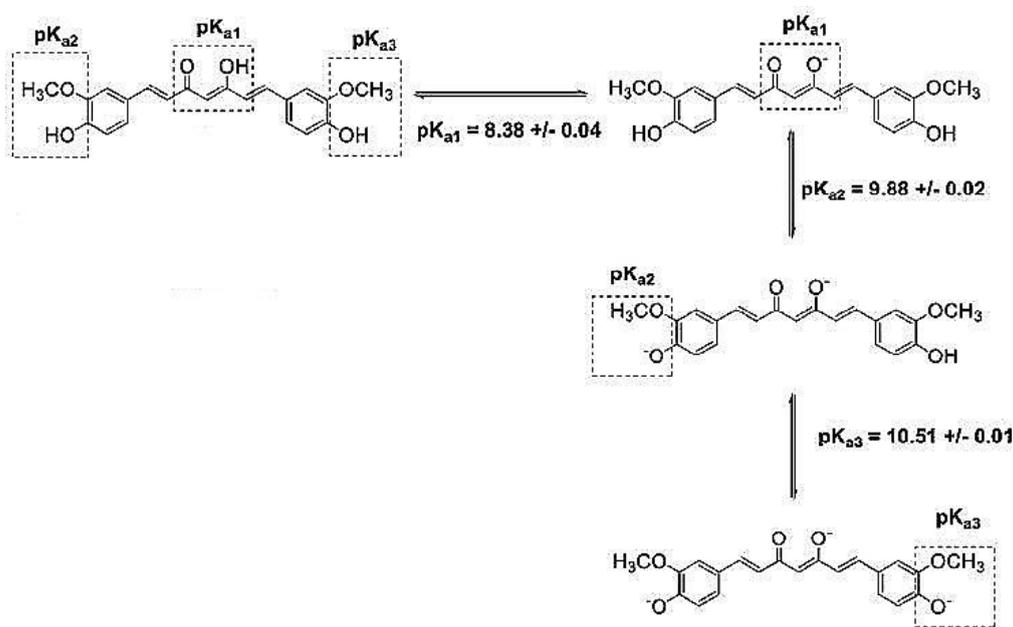
Figure 7. Curcumin deprotonation and according acidity constants (pK_a) [34].

In Table 1. curcumin's main physical and chemical properties are presented.

Table 1. Main physical and chemical properties of curcumin [34].

Physical Description	Orange yellow crystalline powder
Odor	Odorless
Flammability	Non-flammable
Molecular Weight	368.38 g mol^{-1}
Chemical Formula	$C_{21}H_{20}O_6$
Density	0.93 g cm^{-3}
Solubility	Soluble in Polar aprotic solvents

2.6.2. Spectroscopic Properties

Curcumin possesses good photostability, and for its detection, absorption detectors in the wavelength range from 350 to 450 nm range or in the UV region using a common detection wavelength in the range of 250 to 270 nm are usually employed [37]. Furthermore, curcumin's absorption and fluorescence properties provide information on the interaction of curcumin with various micro-heterogenous systems, and its unique absorption spectroscopic properties have already been employed to identify and quantitatively estimate trace elements [2,3,35-38]. Absorption spectrum of curcumin shows two strong absorption bands, one in the visible region with maximum ranging from 410 to 430 nm, and another band in the UV region with maximum around 265 nm, which depend on the used solvent (Table 2.) [34,37]. In general, use of UV–Vis and fluorescence spectroscopy for curcumin quantification has several advantages, including speed and convenience of measurement thanks to the use of a simple calibration curve, but furthermore, these analytical techniques have a high sensitivity for assessing and obtaining data for curcumin in a variety of matrixes [34].

Table 2. Maximums of absorbance in visible region according to used solvent. [34]

Solvent	Maximum Absorption (λ_{max}) / nm
Acetonitrile	422
Dimethylsulfoxide	430
Ethanol	430
Methanol	430
Toluene	420

3. EXPERIMENTAL PART

3.1. MATERIALS AND CHEMICALS

The chemicals required for buffer preparation are given in Table 3.

Table 3. List of chemicals and corresponding formulas for the preparation of buffer solutions.

Citric acid buffer (pH range 2 – 5)		
A	B	Formula
Disodium citrate (0.1 M) or 21.01 g/L of Citric acid monohydrate + 200 mL NaOH (1.0 M)	HCl (0.1 M)	x A + (100-x) B
Phosphate buffer (pH range 5 – 8)		
KH_2PO_4 (0.067 M or 9.073 g/L)	Na_2PO_4 (0.067 M) or Na_2HPO_4 x 2 H2O (11.87 g/L)	x A+ (100-x) B
Citric, Phosphoric and Boric acid buffer (pH range 8 – 13)		
100 mL Citric acid (0.33 mol/dm^3) + 100 mL H_3PO_4, (0.33 mol/dm^3) + 3.54 g Boric acid + 343 mL NaOH (1 M) in 1 L	HCl (0.1 M)	20 mL A + x mL B in 100 mL

Chemicals for preparation of stock solutions and sol-gel precursors:

- ❖ Curcumin, *Fisher Chemical*
- ❖ Tetraethyl orthosilicate (TEOS), *Sigma Aldrich*
- ❖ Ethyl alcohol (96%)
- ❖ Hydrochloric acid (0.1 mol / dm^3)

Other materials used:

- ❖ Glass microscope slides
- ❖ Filter paper

3.2. INSTRUMENTS

- ❖ pH meter MA 5740, *Iskra*
- ❖ Spin-Coater KW-4A, *Chemat Technology Inc.*
- ❖ UV–Vis Spectrophotometer, *Shimadzu*
- ❖ Flame Series Spectrometer + DH-2000-BAL light source, *Ocean Optics*
- ❖ RPH Reflection probe, *Ocean Optics*
- ❖ Ultrasonic bath

3.3. PREPARATION OF REAGENTS

3.3.1. Preparation of Buffer Solutions

Different buffer solutions were prepared for different pH ranges: citric acid buffer was prepared for pH range 2–5, phosphate buffer was prepared for pH range 5–9, and lastly, combination of citric, phosphoric and boric acid was used to prepare buffer solution for pH range 8 – 13. To make the buffer solutions, according to table 1., adequate volumes of solutions A and B were added to 100 mL measuring flask, the flask was filled with distilled water until mark, and mixed. The buffer solution was then transferred in a plastic bottle and its final pH values were determined with a pH meter MA 5740, *Iskra*. All chemicals were of analytical reagent grade and they were used without any further purification, while aqueous solutions were prepared with deionized distilled water.

3.3.2. Preparation of Stock Solutions and Sol-Gel Solutions

To save preparation time, conserve materials and improve the accuracy of working with lower concentration solutions the stock solutions of curcumin were prepared. The first 2 curcumin stock solutions, Stock 1 (5×10^{-2} M) and Stock 2 (1.25×10^{-2} M), were prepared for thin film fabrication on glass slides by dissolving adequate amount of curcumin in 95% EtOH, followed by sonication in an ultrasonic bath for 10 min. The Stock 1 solution was used for preparation of sol-gel mixtures for fabrication of glass thin films with curcumin concentration in the range from $5 \times 10^{-6} - 1 \times 10^{-4}$, while the Stock 2 solution was used for fabrication of thin films in the 1×10^{-4} M $- 1 \times 10^{-2}$ M curcumin concentration range (Table 4.).

Table 4. Composition of sol–gel mixtures used for preparation of glass thin films:

a) with 5×10^{-2} M curcumin stock solution

c(curcumin)/ M	V(Stock 1)/ mL	V(TEOS)/ mL	V(EtOH)/ mL	V(HCl)/ mL
5×10^{-6}	0.03	1	1.2	0.4
1×10^{-5}	0.06	1	1.2	0.4
5×10^{-5}	0.30	1	1.2	0.4
1×10^{-4}	0.60	1	1.2	0.4

b) with 1.25×10^{-2} M curcumin stock solution

c(curcumin)/ M	V(Stock 2)/ mL	V(TEOS)/ mL	V(EtOH)/ mL	V(HCl)/ mL
1×10^{-4}	0.02	1	1.2	0.4
5×10^{-4}	0.11	1	1.2	0.4
1×10^{-3}	0.23	1	1.2	0.4
5×10^{-3}	1.73	1	1.2	0.4
1×10^{-2}	10.40	1	1.2	0.4

c) with 1.25×10^{-2} M curcumin stock solution.

c(curcumin)/ M	V(Stock 2)/ mL	V (TEOS)/ mL	V (EtOH)/ mL	V (HCl)/ mL
2×10^{-3}	0.99	2	2.4	0.8
4×10^{-3}	2.45	2	2.4	0.8
6×10^{-3}	4.80	2	2.4	0.8
8×10^{-3}	9.24	2	2.4	0.8
1×10^{-2}	20.80	2	2.4	0.8

Another stock solution, Stock 3 (4.17 x 10^{-3} M), was prepared from Stock 2, and was used for fabrication of curcumin-based paper strips, for 3 different concentrations of curcumin: 1 x 10^{-5} M, 1 x 10^{-4} M, and 1 x 10^{-3} M (Table 5.).

Table 5. Composition of sol–gel mixtures used for preparation of paper strips (4,17 x 10^{-3} M curcumin Stock 3 solution).

c(curcumin)/ M	V(Stock 3)/ mL	V (TEOS)/ mL	V (EtOH)/ mL	V (HCl)/ mL
$1,0 \times 10^{-5}$	0.0288	5	5	2
$1,0 \times 10^{-4}$	0.2880	5	5	2
$1,0 \times 10^{-3}$	2.8800	5	5	2

To easily differentiate between curcumin concentrations in sol-gels on paper strips, in further text they will be referred to as:

- o Low C.S. (1.0×10^{-5}),
- o Middle C.S. (1.0×10^{-4}), and
- o High C.S. (1.0×10^{-3}).

3.4. SENSOR FABRICATION

3.4.1. Curcumin-Based Glass Thin Films

Stock 1 and 2 solutions were used for fabrication of pH sensitive thin films on glass slides, and sol-gel solutions were prepared according to Table 5. In the first 2 series, sol-gel solutions were made by mixing 1 mL of TEOS, 2.4 mL of ethanol, 0.8 mL of 0.1 M HCl and an adequate volume of the curcumin stock solution to make the desired concentrations (Table 4.a,b). In the third series, sol-gel mixtures were prepared in the same manner, but with doubled volumes of TEOS, ethanol, and HCl (Table 4.c). All solutions were homogenized in an ultrasonic bath for 15 min after which they were stored in the dark at room temperature and left for 3 days to age. The pH sensitive thin films were prepared by spin coating 100 µL of the aged solutions onto 25 mm × 25 mm × 1 mm glass microscope slides using a commercial spin-coater (KW-4A, *Chemat Technology Inc.*). The glass substrates were rotated at 3,500 rpm for 30 s. Prior to film deposition, the glass substrates had been treated with concentrated nitric acid for 30 min in order to activate the silanol groups on the surface of the glass. Afterwards, slides were rinsed with ethanol and distilled water, and dried at 100 °C for 30 min. After coating, films were left for 5 days to dry at room temperature before optical characterization.

3.4.2. Curcumin-Based Paper Strips

Curcumin-based paper strip fabrication followed an easier pathway. Sol-gel mixtures were prepared according to Table 5., and 40 µL of aged sol-gel solution was dropped onto 2×2 cm^2 filter paper and left to dry at room temperature. After 3 days, their optical properties were measured.

3.5. OPTICAL CHARACTERIZATION

Optical characterization of sol-gel solutions and glass thin films included absorbance measurements, while for paper strips reflectance was measured, and curcumin's signature in the visible range (360–750 nm) was explored. Absorption spectra were determined with a UV–Vis Spectrophotometer, while Flame Series Spectrometer with an external light source DH-2000-BAL was used for reflectance measurement of paper strips. For reflectance measurements, reflectance probe was used to deliver electromagnetic radiation from the source to the detector.

3.5.1. Absorbance Measurement

The range of measurement was from 310 nm to 610 nm. Absorbance of glass slides, prepared according to the Table 4., was measured. Thin film with 0.01 M curcumin concentration showed the best results so it was chosen for pH characterization. Each film with 0.01 M curcumin concentration was immersed in 5 mL of buffer solution in pH range 2 - 10 for 1 min, and after drying, it was placed upright in Spectrophotometer extension, so that the incident light passes directly through the middle of the glass. Absorption spectra of curcumin solution in pH range from 2 to 13 were also measured. 3.5 mL of each buffer solution was added to a cuvette, followed by 8.4 µL of Stock 3 solution right before screening, making the final concentration of 1.0×10^{-5} M. The cuvette was covered, shaken and absorbance was measured after 1 min stabilization.

3.5.2. Reflectance Measurement

The range of measurement was from 400 nm to 800 nm. Some of the settings in the spectrometer were as follows to provide a smooth spectrum by lowering measurement noise: the averaging was set at 35 (number of internal scans taken to compute the mean spectrum), and boxcar-width (similar to moving average) as 5. The sample was illuminated and the reflected light from the sample was collected using a single reflectance probe with two connectors (one for the light source and one for the spectrometer). As a reference standard, clean filter paper

was used. Reflectance measurement involved dropping 80 μ of buffer solution (pH = 2 – 13) on previously prepared paper strips, letting it to dry for 45 min at room temperature, and finally filming the reflectance. Both absorbance and reflectance measurements were made within 2 weeks of glass film and paper strip fabrication and were not preconditioned prior to measuring their response times.

3.6. STABILITY TEST

Stability testing was utilized to determine if the quality of a sensory part, in other words immobilization of curcumin, is altered over time. Testing was done for both curcumin in EtOH and curcumin in sol (Low, Middle, and High C.S.) by submerging the (same) paper strip in buffer solution of pH 6, 8, 10, 12, and 13, for 2 min. After drying for 45 min at room temperature, reflectance of paper strips was measured. Testing was repeated multiple times for t = 1, 2, 3, 4, 5, and 6 min.

3.7. REVERSIBILITY TEST

Reversibility testing was employed to determine the repeatability of the sensory part after exposing paper strips to buffer solutions of 2 different pH = 6 and 10, and reversibility was tested for both curcumin in EtOH and in sol (High C.S.) in 5 cycles. First, the (same) paper strip was submerged in buffer solution of pH 6 for 3 min, and after drying for 45 min at room temperature, reflectance of paper strips was measured. The same procedure was then repeated, but the paper strip was submerged in the buffer solution of pH 10, and with it the first cycle was complete. The whole process was then repeated for 4 more times, equaling to 5 cycles of pH change.

4. RESULTS AND DISCUSSION

4.1. CURCUMIN-BASED GLASS THIN FILMS

4.1.1. Determination of Curcumin Concentration Range

In the first series, sol-gel solutions were prepared according to Table 4.a, with curcumin in concentration range from 5×10^{-6} - 1×10^{-4} M, and were spin coated on glass substrates, but the films were transparent and not applicable for further characterization, so in the second series, more concentrated sol-gel mixtures were made, with curcumin concentration 1×10^{-4} - 1×10^{-2} M (Table 4.b), and their absorbance was recorded (Figure 8.).
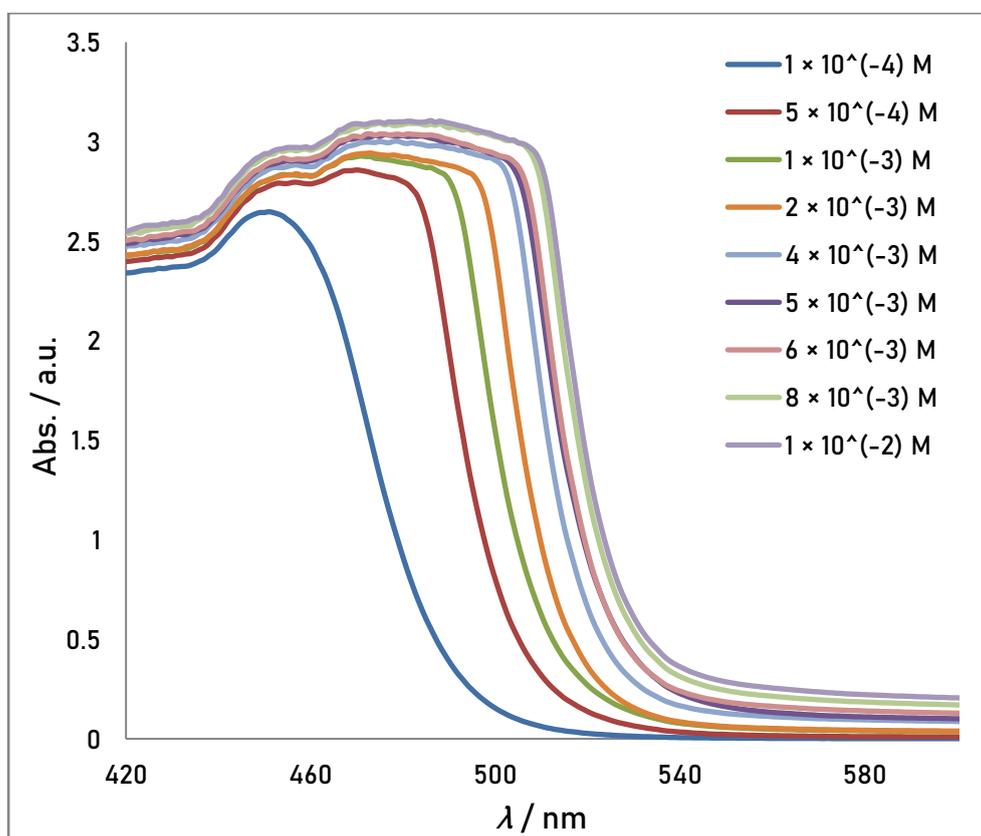
Figure 8. Absorbance spectra of sol-gel solutions with curcumin concentration $c = 1 \times 10^{-4}$ - 1×10^{-2} M.

Based on Figure 8., sol-gel mixtures with curcumin concentration ranging from $c = 2 \times 10^{-3}$ - 1×10^{-2} M showed the highest and strongest absorbance intensity, providing bright yellow color, and thus were chosen for fabrication of glass thin films. In the next step, curcumin-based glass thin films ($c = 2 \times 10^{-3}$ - 1×10^{-2} M) were prepared according to previously described method (3.4.1.) and their absorbance was measured 5 days after fabrication (Figure 9.).
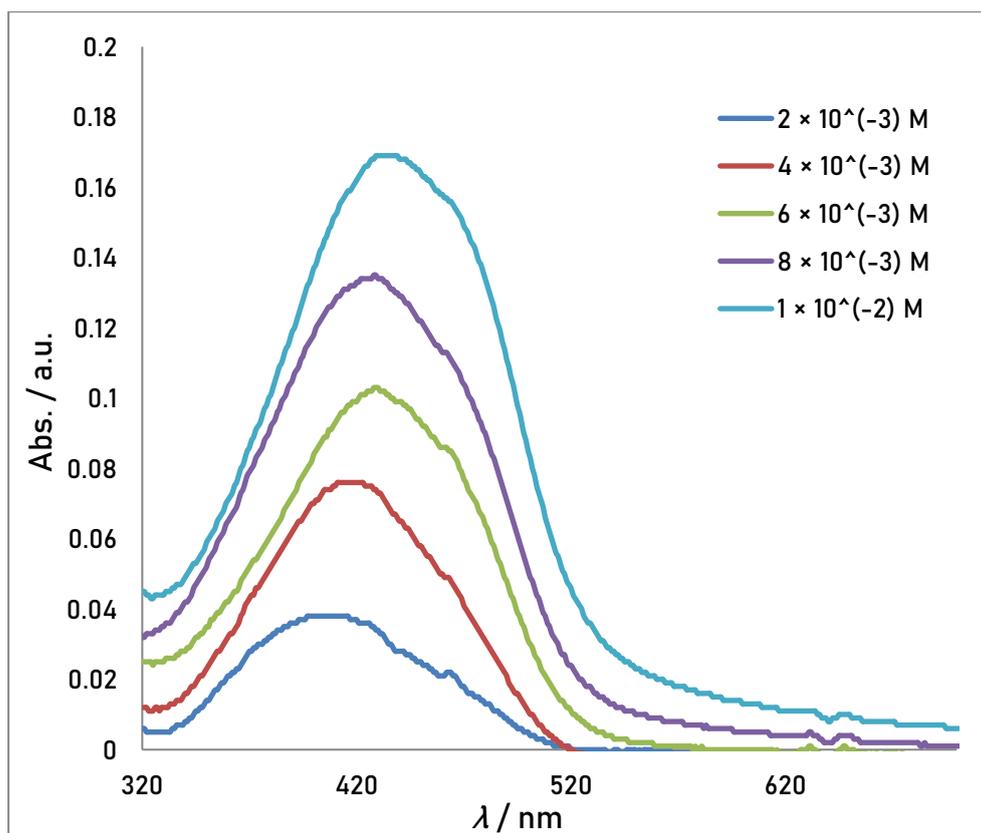
Figure 9. Absorbance spectra of curcumin-based glass thin films with curcumin concentration $c = 2 \times 10^{-3}$ - 1×10^{-2} M.

All thin films showed an absorbance maximum in the range between 400 and 430 nm, which can be assigned to the lowest $\pi - \pi^*$ transitions occurring in curcumin, representing absorbance in the violet region and transmittance of light in a yellow region [35,36]. Furthermore, as the concentration of curcumin increased, bathochromic shift, followed by hypsochromic shift, was noticed, so curcumin-based glass thin film with the

highest concentration of curcumin ($c = 1 \times 10^{-2}$ M) was chosen for further characterization due to the best colorization.

4.1.2. pH Characterization

Absorbance spectra of curcumin-based glass thin films ($c = 1 \times 10^{-2}$ M) were recorded at pH = 2.2 – 10.0. The results are presented on Figure 10.
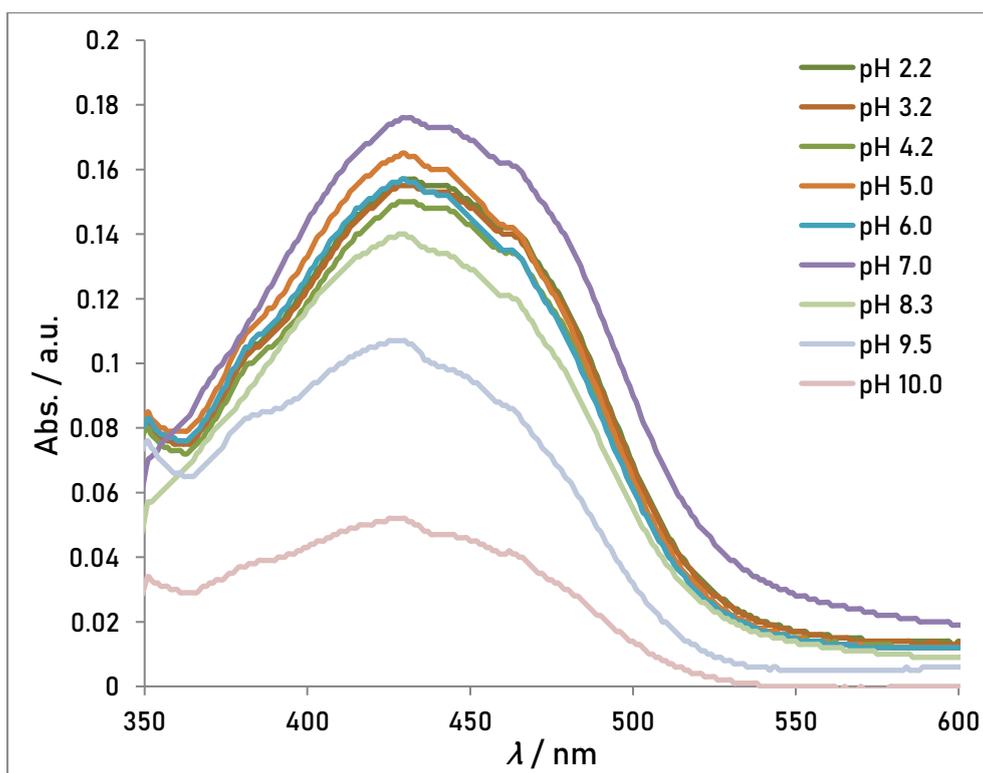
Figure 10. pH characterization of curcumin-based glass thin films ($c = 1 \times 10^{-2}$ M).
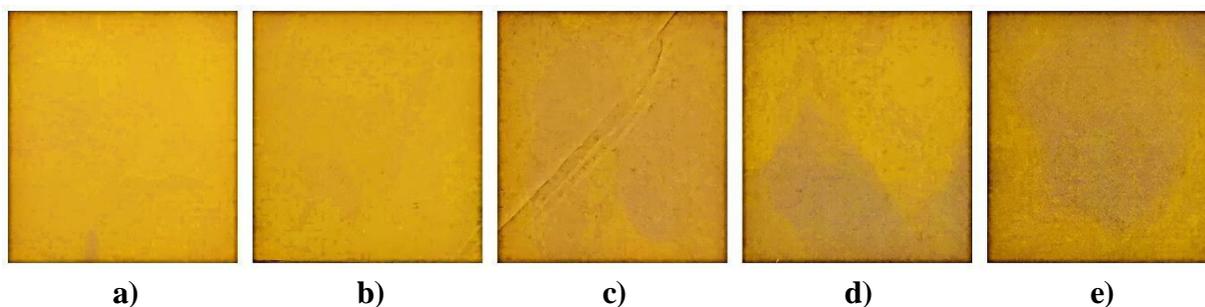
Figure 11. Visual representation of curcumin-based thin films ($c = 1 \times 10^{-2}$ M) used at:
a) pH 4.6, b) pH 6.6, c) pH 8.7, d) pH 9.5, and e) pH 10.0.

Initially, characterization of glass thin films was meant to be done up to pH 13, but after 7.0 pH, absorbance intensity started to rapidly decrease at 433 nm, as shown on Figure 10., and 11., so further measuring was stopped at pH 10.0 because curcumin was leaking out to the buffer solution. Suspected reason for curcumin poor stability on glass thin films is that curcumin is more soluble in ionic form (deprotonated) which is present in basic medium, thus it escapes from the TEOS matrix. Loss of colorization was calculated as a relative intensity difference between pH 2.0 and given pH (Figure 12. and Table 6.).
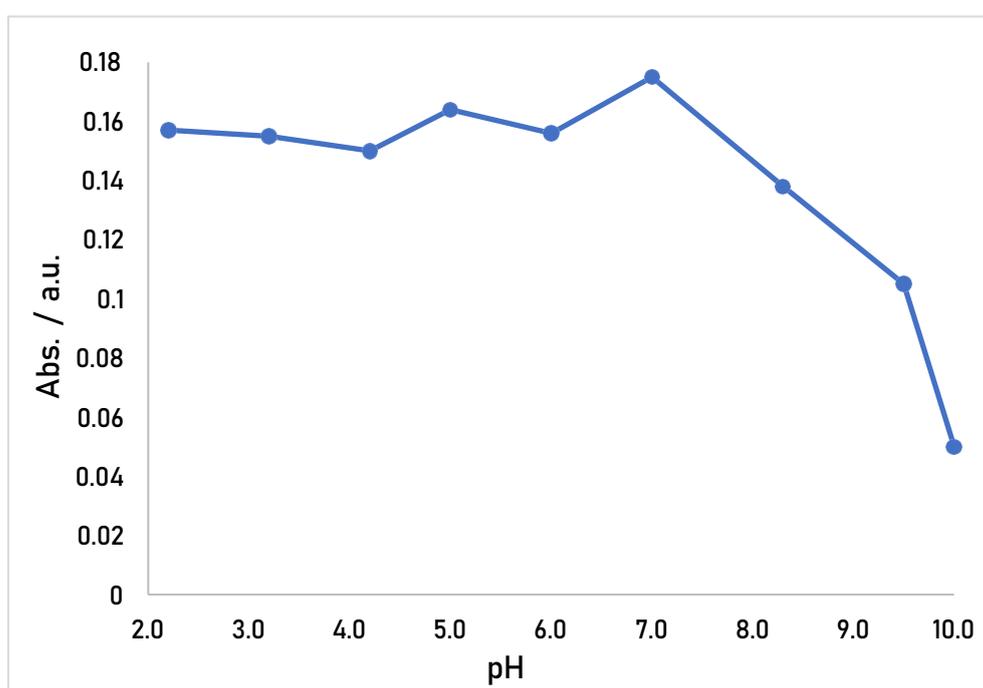
Figure 12. Intensity of curcumin-based glass thin films ($c = 1 \times 10^{-2}$ M) at 433 nm in the pH range 2 – 10.

Table 6. Loss of colorization of curcumin-based glass thin films ($c = 1 \times 10^{-2}$ M) according to pH

pH	Loss of colorization/ %
8.3	13
9.5	38
10.0	70

As can be seen in Table 6., curcumin-based thin film resulted in 70% loss of colorization at pH 10.0, so no further experiments were conducted with thin films on glass slides, and filter paper was chosen as an alternative.

4.2. CURCUMIN-BASED PAPER STRIPS

4.2.1. Behavior of Curcumin + EtOH Solution at pH 2 – 13

In order to determine the possibility of using curcumin as an optical pH sensor, the change in its spectral properties depending on the pH value of the solution was examined. Solutions of curcumin samples in acidic and neutral conditions were colored yellow, but in alkaline medium the color of solutions first changed from yellow to red, then to brownish-orange, as seen in Figure 13.
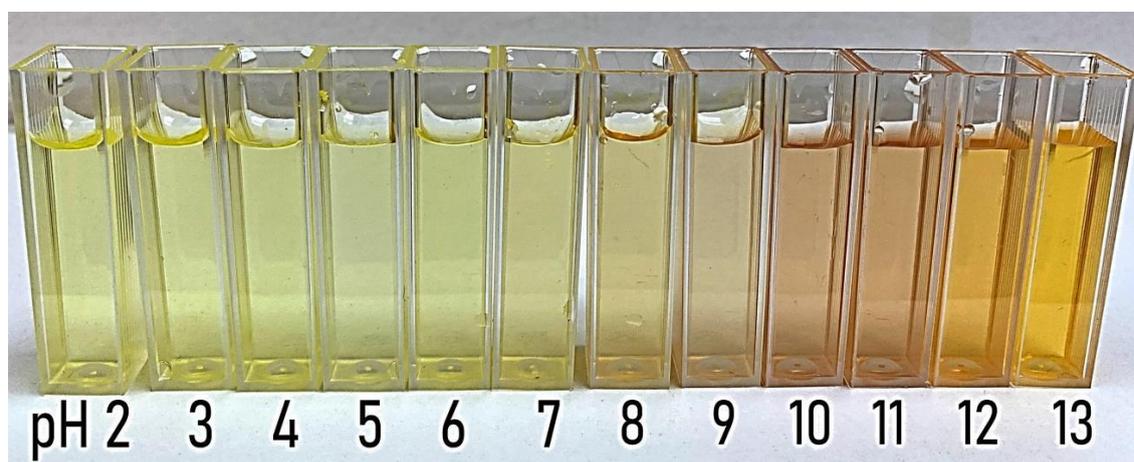
Figure 13. Color change of curcumin solution ($c = 1.0 \times 10^{-5}$ M) in EtOH (96%), in buffer solutions of different pH (pH = 2 - 13).

4.2.2. pH Characterization of Curcumin + EtOH Solution

Absorption spectra of curcumin solution ($c = 1.0 \times 10^{-5}$ M) in EtOH (96%) in citric acid buffer (pH = 4 – 5), phosphate (pH = 5 – 8), and citric, phosphoric and boric acid buffer (pH = 8 – 13) solutions were recorded according to the previously described procedure (3.5.1.), and the results are presented on Figure 14.

Up to pH = 7, the spectra of curcumin in EtOH remain very similar without considerable change in intensity of absorbance, meaning that curcumin form in acidic and neutral conditions is the same and stable. At higher pH values, curcumin's behavior changes (Fig. 14.a). To get a better understanding, and a better visual representation of the noticed changes above pH 7, absorption spectra were divided into two pH regions: a) pH = 7 – 10, and b) pH = 10 – 13 (Fig. 14.b, c).
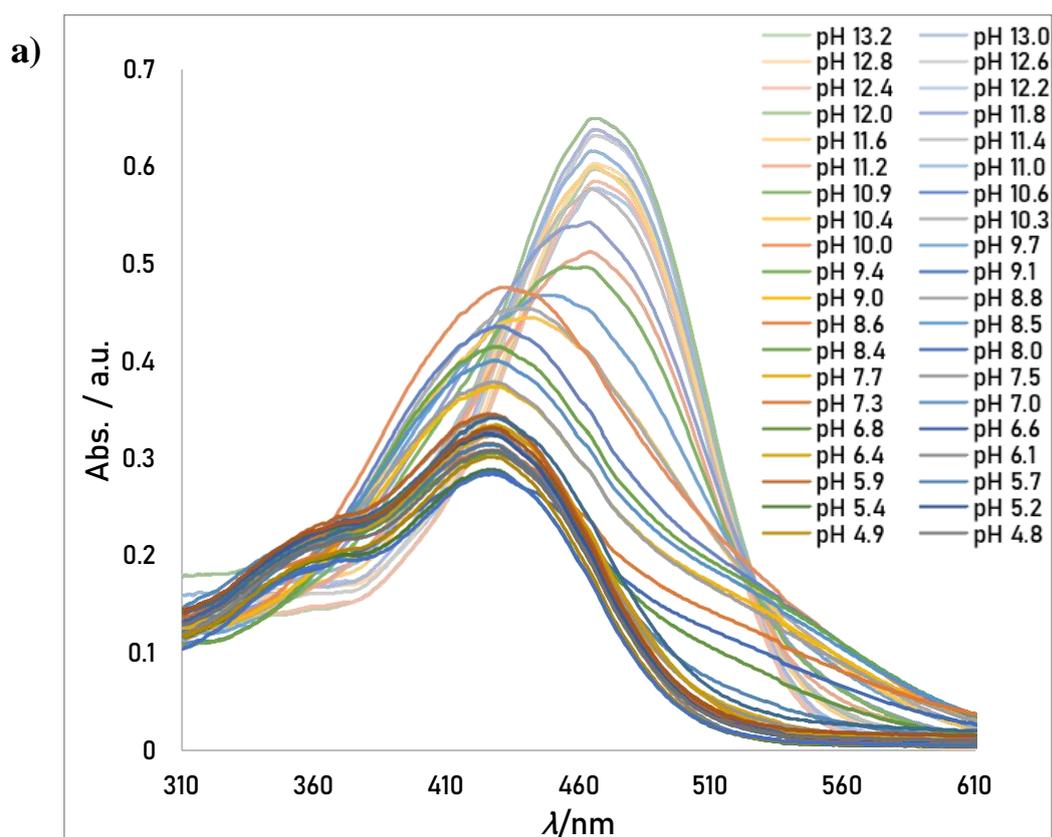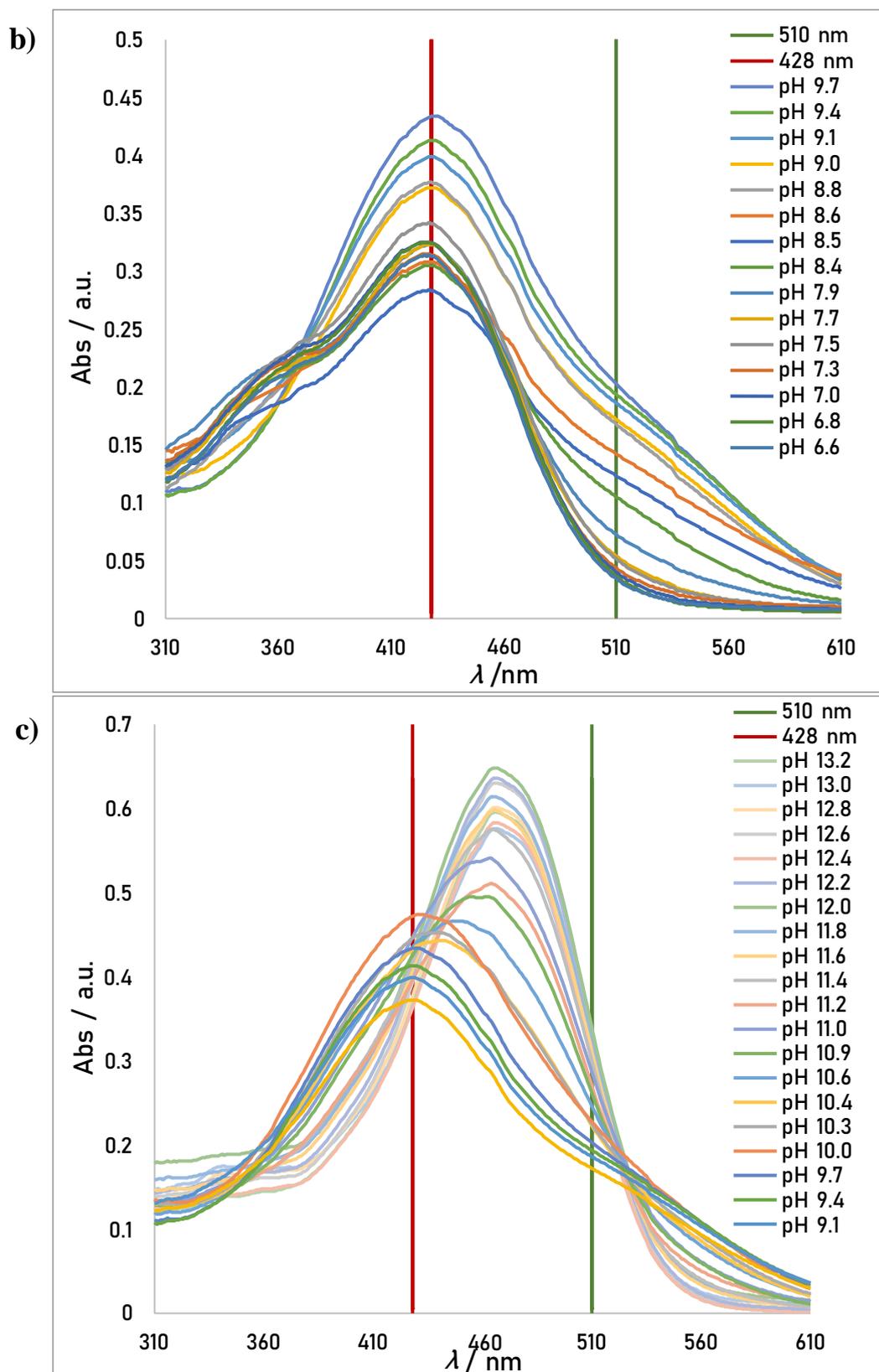
Figure 14. UV-Vis absorption spectra of curcumin solution ($c = 1.0 \times 10^{-5}$ M) and EtOH (96%), in different buffer solutions for: a) pH = 4 – 13, b) pH = 7 – 9, and c) pH = 9 – 13.

As seen on Figure 14., curcumin dissolved in EtOH (96%) exhibits strong absorption with the maximum absorption at $\lambda = 428$ nm in acid and neutral environment, while in alkaline media the absorption maximum is observed at 467 nm, which is in agreement with the literature data [2,47,48]. The maximum absorption is due to the electronic dipole allowed π-π* type excitation of its extended conjugation system [49]. The yellow color of curcumin solution in acidic and neutral pH region is in correlation with the given UV-Vis absorbance spectra, meaning that at 428 nm curcumin solution absorbs in violet region, and emits yellow color, as previously seen on Fig.13. Looking at Fig. 14.b, at $\lambda = 510$ nm, from pH = 7.9 there is a significant increase of absorbance, indicating the start of a color change to darker yellow, but the most significant color change is noticed at higher pH values. Looking at Fig. 14.c, from pH = 10.0 a bathochromic (red) shift is noticed, which is followed by hyperchromic shift, meaning that conjugation in the chromophore (curcumin) is increased.

The red shift is better depicted on Figure 15., where the data is normalized to provide a clearer representation of peaks moving in a direction of higher wavelengths. The exact maxima of wavelengths at each pH in basic medium are shown in Table 7. Similar values were established by other studies as well, confirming a red shift at about 467 nm under basic conditions (pH > 10), which is reflected in the change of color from red to brownish-orange (Fig. 13.) [47,48,50].
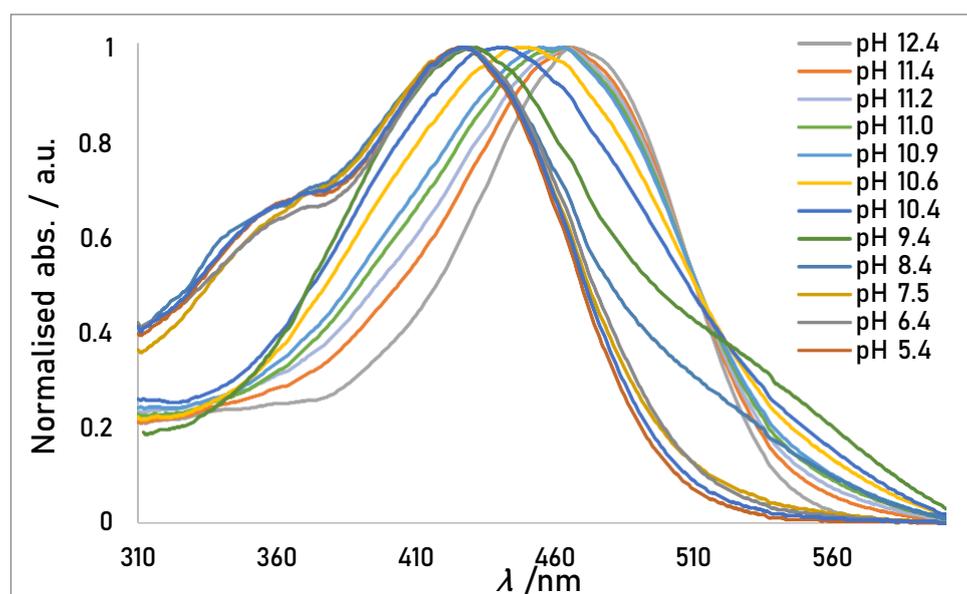
Figure 15. Normalized graph of UV-Vis absorption spectrum of curcumin solution ($c = 1.0 \times 10^{-5}$ M) in EtOH (96%) in pH = 4 − 12.

Table 7. UV-Vis absorbance maxima (λ_{max}) of curcumin solution ($c = 1.0 \times 10^{-5}$ M) in EtOH (95%) in pH = 9 – 13.

pH	9.38	10.04	10.40	10.87	11.23	11.60	12.00	12.40	12.80	13.20
λ_{max} / nm	428	434	439	459	464	466	466	466	468	467

Presented results are in agreement with the literature data according to which the yellowish color of curcumin solution in acidic and neutral media is caused by absorption of curcumin in its keto form, while in alkaline media more conjugated enol form dominates, which is responsible for the red and brownish-orange color of the solution at higher pH [3,48]. Furthermore, Anjomshoa et al. reported that in aqueous solutions, curcumin's favorable form is enol form because of strong intramolecular hydrogen bond which provides greater stability [51].

4.2.3. pK_a Value Determination

In this study, two pK_a values of the curcumin solution in aqueous media have been determined, following the changes on the UV-Vis spectra as a function of pH. At $\lambda = 510$ nm, between pH = 7.9 and 8.4 (Fig.14.b), a high jump in intensity can be observed, suggesting the first pK_{a1} value, while the second intensity increase can be observed on Fig. 14.c, between pH = 9.1 and 11.0, indicating the second pK_{a2}. Since absorption spectra were divided into two pH regions, two sigmoidal curves were created. Ratio in absorption at two different wavelengths was used to provide the response independent of concentration, and the graphs are represented in Fig. 16. The inflection point on both graphs corresponds to pK_a values which were calculated by Boltzmann model. For the first pH range (pH = 7 – 9) the calculated value equals pK_{a1} = 8.20, while for the second range (pH = 9 – 13) equals pK_{a2} = 11.04 with R^2 = 0.99 in both cases, respectively. Similar pK_a values were established by other studies, attributing the pK_{a1} to dissociation of enol proton, and pK_{a2} to dissociation of phenolic proton [47,48,50,52].

a)

Model	Boltzmann		
Equation	y = A2 + (A1-A2)/(1 + exp((x-x0)/dx))		
Reduced Chi-Sqr	3,40516E-4		
Adj. R-Square	0,98575		
		Value	Standard Error
ratio 510/427	A1	0,12597	0,00913
ratio 510/427	A2	0,47704	0,00893
ratio 510/427	x0	8,20427	0,03546
ratio 510/427	dx	0,2228	0,02985

b)

Model	Boltzmann		
Equation	y = A2 + (A1-A2) /(1 + exp((x-x0) /dx))		
Reduced Chi-Sqr	4,57567E-5		
Adj. R-Square	0,99793		
		Value	Standard Error
ratio 510/427	A1	0,45871	0,0039
ratio 510/427	A2	0,82953	0,00343
ratio 510/427	x0	11,03551	0,01872
ratio 510/427	dx	0,40324	0,01769

Figure 16. Sigmoidal pH titration curves for a) pH = 7 − 9, and b) pH = 9 − 13.

4.2.4. Isosbestic Point

In this study, one prominent isosbestic point was noticed at $\lambda = 525$ for pH = 9.7 – 11.8 [48], and is highlighted on Figure 17. Knowing that curcumin has three acidic hydrogens (from one phenolic and 2 enolic groups), which according to its enol form structure, can dissociate, thus this isosbestic point indicates a balance between the dianionic form at pH = 10.0 – 11.0, and the completely deprotonated form at pH = 12.0 which gives rise to a red solution in basic media [48,50,51].
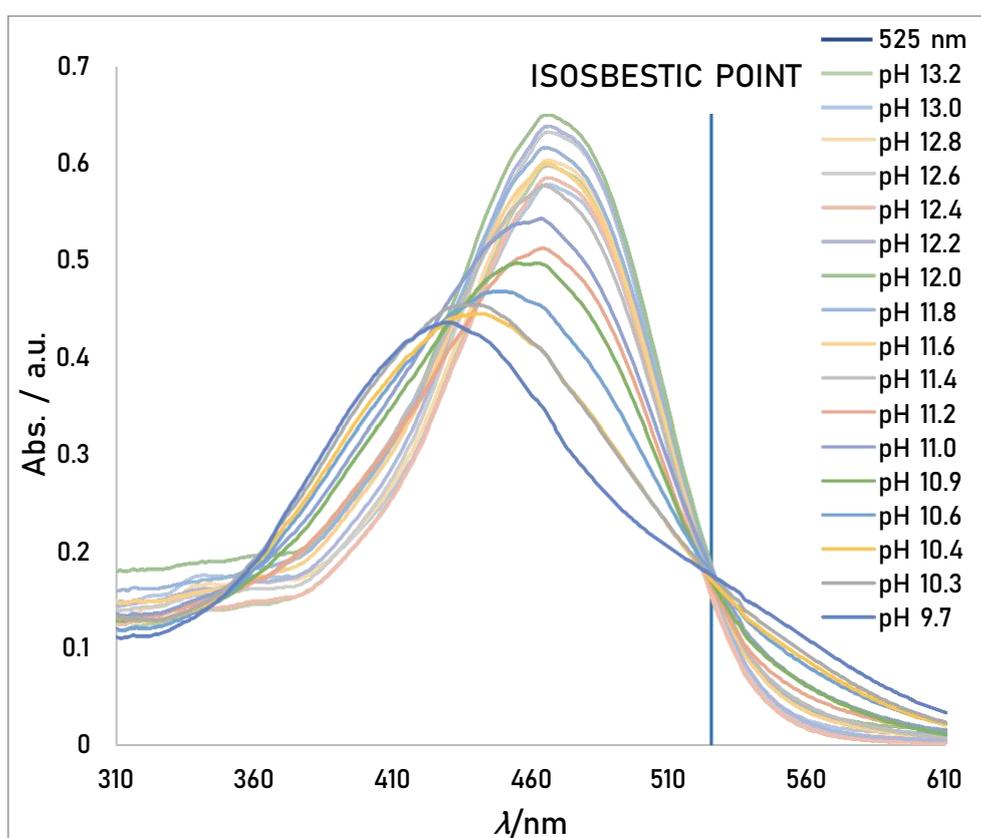
Figure 17. Isosbestic point for curcumin (at 525 nm) at pH = 10 – 12.

4.2.5. Optical Characterization

Spectrophotometric analysis was performed on 2 different types of curcumin-based paper sensors: 1) sensor where the curcumin is dissolved in EtOH and deposited on filter paper, and 2) sensor where curcumin is immobilized on TEOS (by sol-gel method) and deposited on filter paper. Characterization was performed on two systems so that a comparison can be made based on the results, and that the performance of the sensor can be optimized. Furthermore, three sol-gel curcumin-based paper sensors were prepared according to previously described method (3.4.), and are presented on Figure 18.

a)   **b)**   **c)**
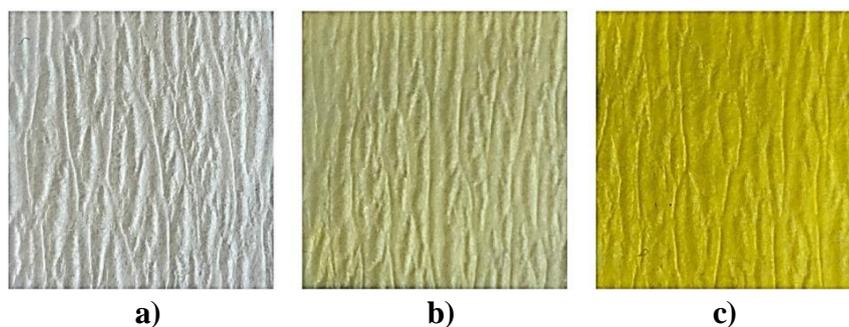
Figure 18. Sol-gel curcumin-based paper sensors: a) Low C.S. ($c = 1.0 \times 10^{-5}$ M),
b) Middle C.S. ($c = 1.0 \times 10^{-4}$ M), and c) High C.S. ($c = 1.0 \times 10^{-3}$ M).

The color of Low C.S. was not strong enough for reflectance measurement so it was left out of further research, while reflectance measurements of Middle C.S. were stopped after pH = 10.0 because the color change was weak due to low concentration of curcumin (Figure 19.). Thus, further research was continued only with High C.S. paper strip.
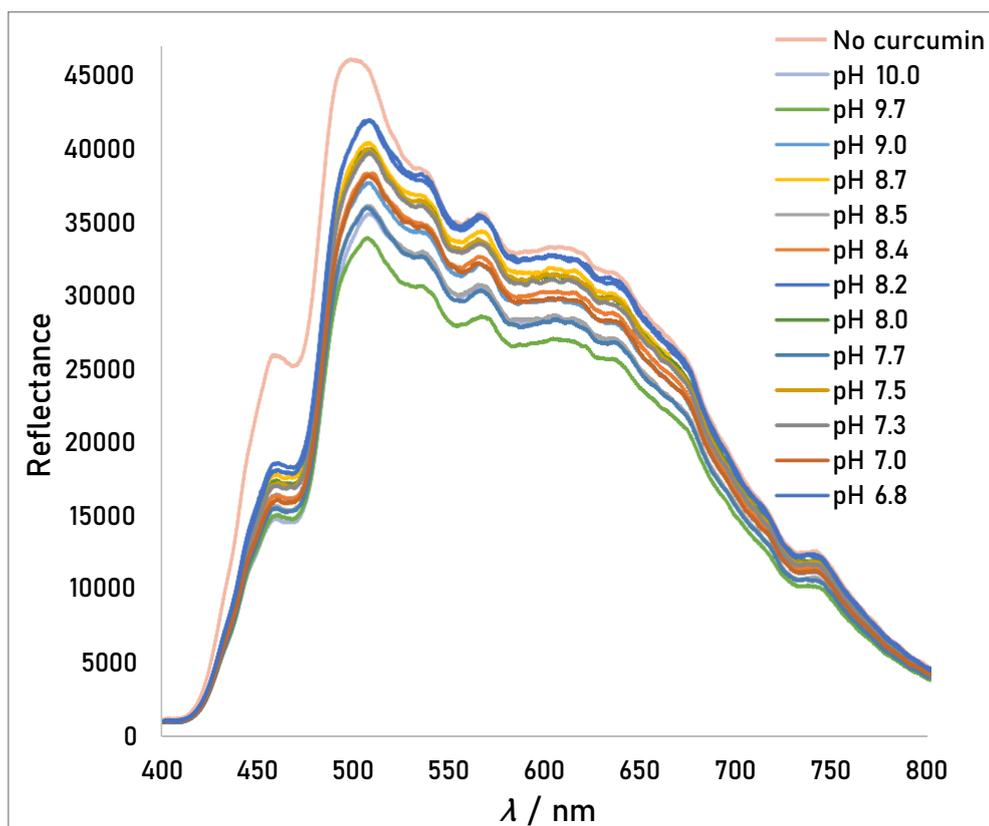
Figure 19. Reflectance spectra of Middle C.S. ($c = 1.0 \times 10^{-4}$ M) paper strip at pH = 7 – 10.

Reflectance spectra of paper sensor with solution of curcumin in EtOH are shown in Figure 20. For better visual presentation the results are divided into 2 graphs depending on the pH range: 1) pH = 7 – 10, and 2) pH = 10 – 13.
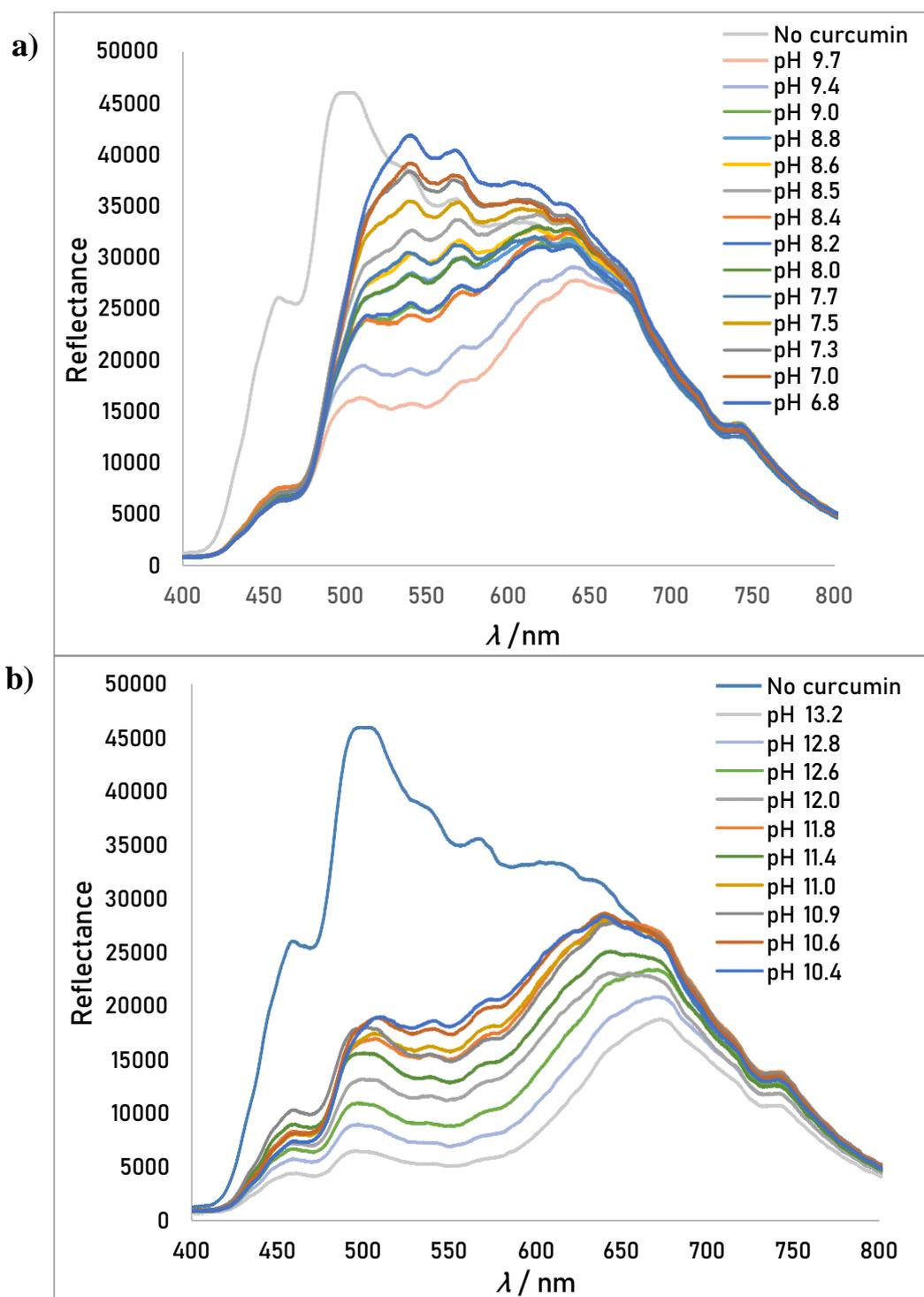
Figure 20. Reflectance spectra of Curcumin + EtOH ($c = 1.0 \times 10^{-3}$ M) paper strip at: a) pH = 7 – 10, and b) pH = 10 – 13.

As in absorbance spectra (Fig. 14,15.), red shift is also seen in reflectance spectra, as presented in Fig 20.a). As the pH increases, intensity of two highest peaks up to pH = 8, λ = 540 and 568 nm, starts going down, while the intensity of a broad peak at 640 nm starts increasing. This change in intensity indicates a color change of paper sensor, from yellow to red and brownish orange, and is in agreement with previous results of measured absorbance. The same behavior can be seen in sol-gel immobilized-curcumin-based paper sensor (Figure 21.).
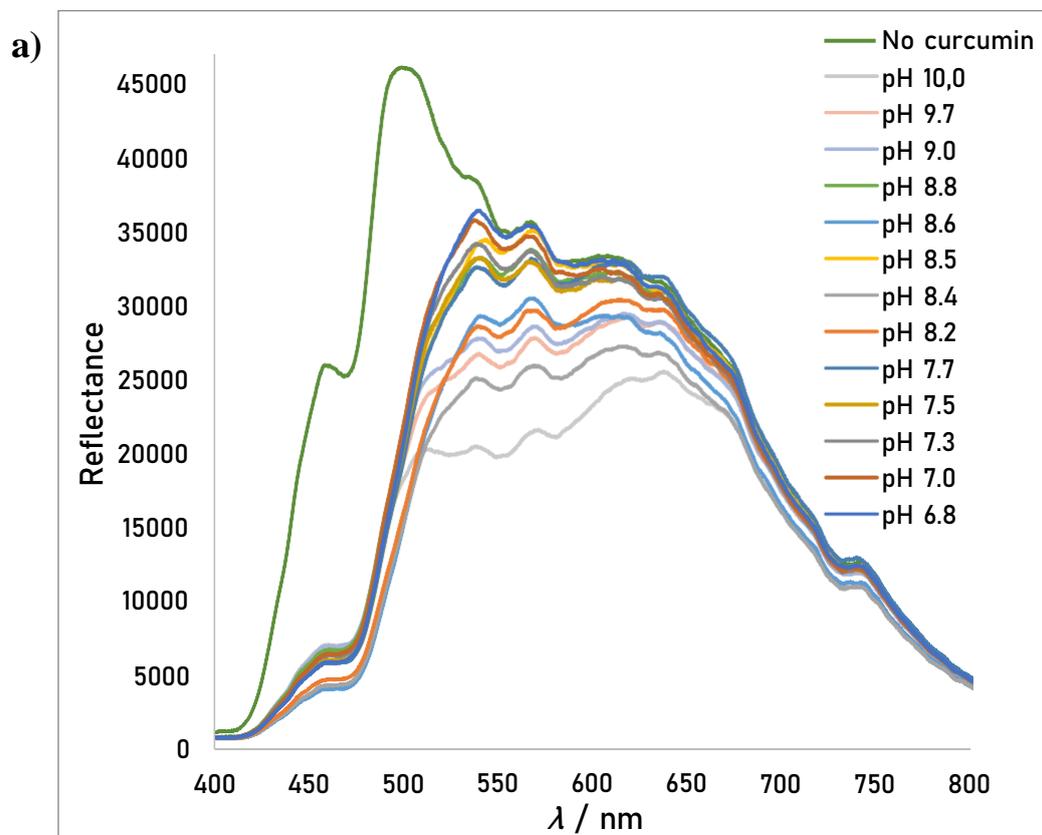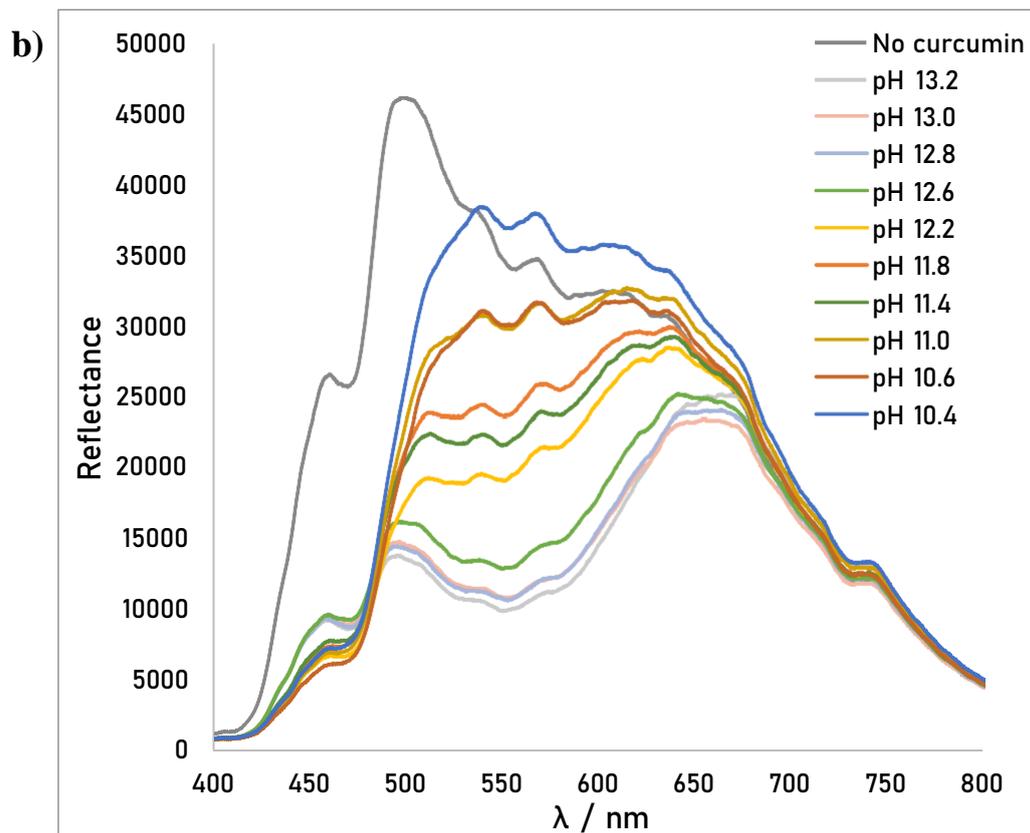
Figure 21. Reflectance spectra of High C.S. ($c = 1.0 \times 10^{-3}$ M) paper strip at:
a) pH = 7 – 10, and b) pH = 10 – 13.

In both cases, for both Curcumin + EtOH and High C.S. paper strips, maximum of reflectance of protonated form of curcumin dye is at $\lambda_{max} = 574$ nm corresponding to all pH up to 7.5, while the reflectance maximum of deprotonated form is at a $\lambda_{max} = 650$ nm from pH = 9.0 – 13.2.

Furthermore, the clearest trend among the output signals (Fig. 20,21.) can be observed at wavelengths of 640 and 540 nm. Considering the ratio of the intensity values at those wavelengths for tested pH values, calibration curves were made and are presented in Figure 22.
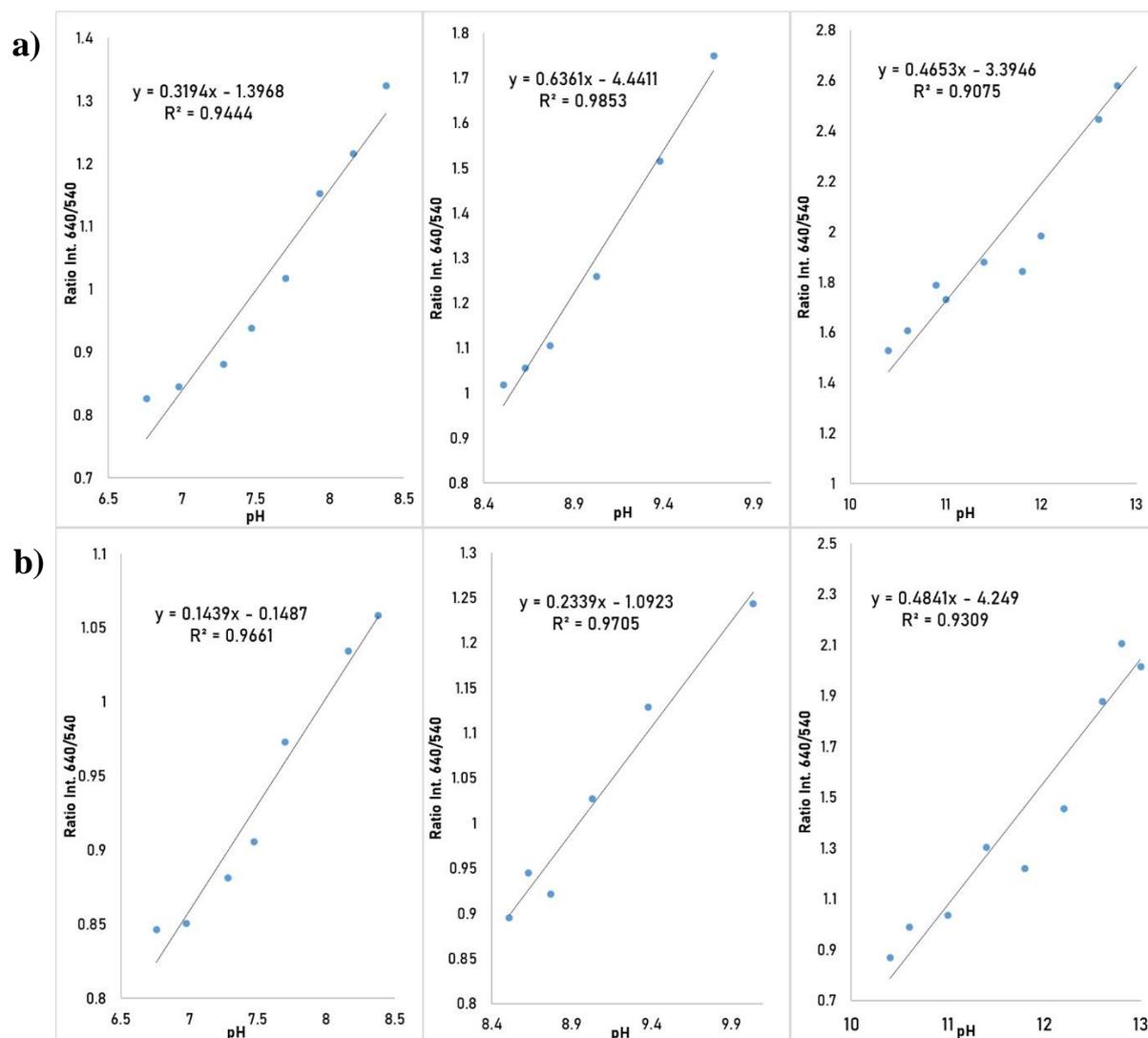
Figure 22. Calibration curves of: a) Curcumin + EtOH ($c = 1.0 \times 10^{-3}$ M) paper strip, and b) High C.S. ($c = 1.0 \times 10^{-3}$ M) paper strip; for pH = 7 – 13.

As seen in Fig. 22, with an increase in pH, the ratio of intensities also increases, going in favor of higher wavelength at 640 nm, which is in correlation with previously established bathochromic shift. Calculated values of correlation coefficients, R^2 and corresponding slopes are shown in Table 8.

Table 8. Calibration curve characteristics (R^2 and slope) of Curcumin + EtOH and High C.S. paper strips in pH range 7 – 13.

a) Curcumin + EtOH ($c = 1.0 \times 10^{-3}$ M) paper strip		
pH	6.5 – 8.5	8.5 – 10.0	10.0 – 13.0
R^2	0.9444	0.9853	0.9075
Slope	0.3194	0.6361	0.4653
b) High C.S. ($c = 1.0 \times 10^{-3}$ M) paper strip		
pH	6.5 – 8.5	8.5 – 10.0	10.0 – 13.0
R^2	0.9661	0.9705	0.9309
Slope	0.1439	0.2339	0.4841

Based on given results (Fig. 22 and Table 8.) the highest increase in intensity for Curcumin in EtOH can be observed between pH 8.5 and 10.0, while for High C.S. the most noticeable color change occurs at higher pH, between 10.0 and 13.0. The same conclusion was acquired by visual inspection (Figure 23.), which can be attributed to immobilization of curcumin in the silica network, making a barrier for buffer solution and making it harder for it to reach the curcumin dye.
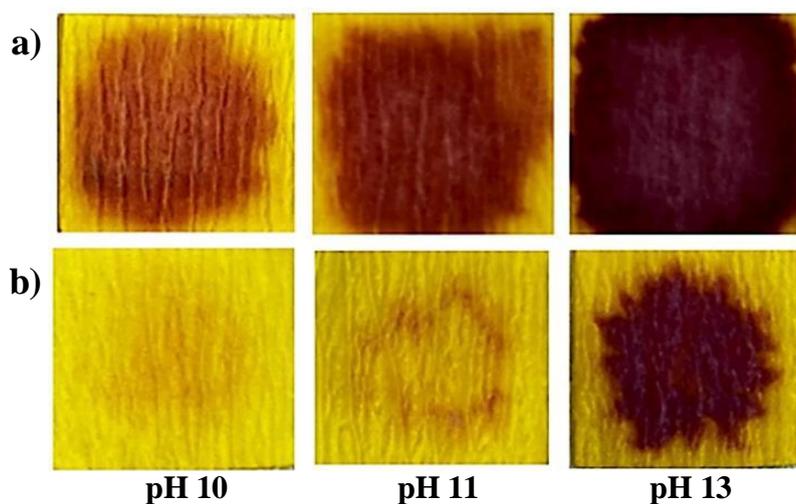
Figure 23. Visual representation of paper strips a) Curcumin + EtOH ($c = 1.0 \times 10^{-3}$ M), and b) High C.S. ($c = 1.0 \times 10^{-3}$ M), in pH = 11, 12, and 13.

4.2.6. Stability Performance

Since curcumin is stable when kept in acidic condition, and the color degradation occurs at alkaline condition, stability testing was done in pH range 6 – 13 according to previously described procedure (3.6). Based on previous research, the highest change was noticed at 640 nm, so graphs were plotted with the intensity at that wavelength over a time frame of 12 min all together, with measurements done in 6 intervals, each after 2 min stabilization (Figures 24,25.).
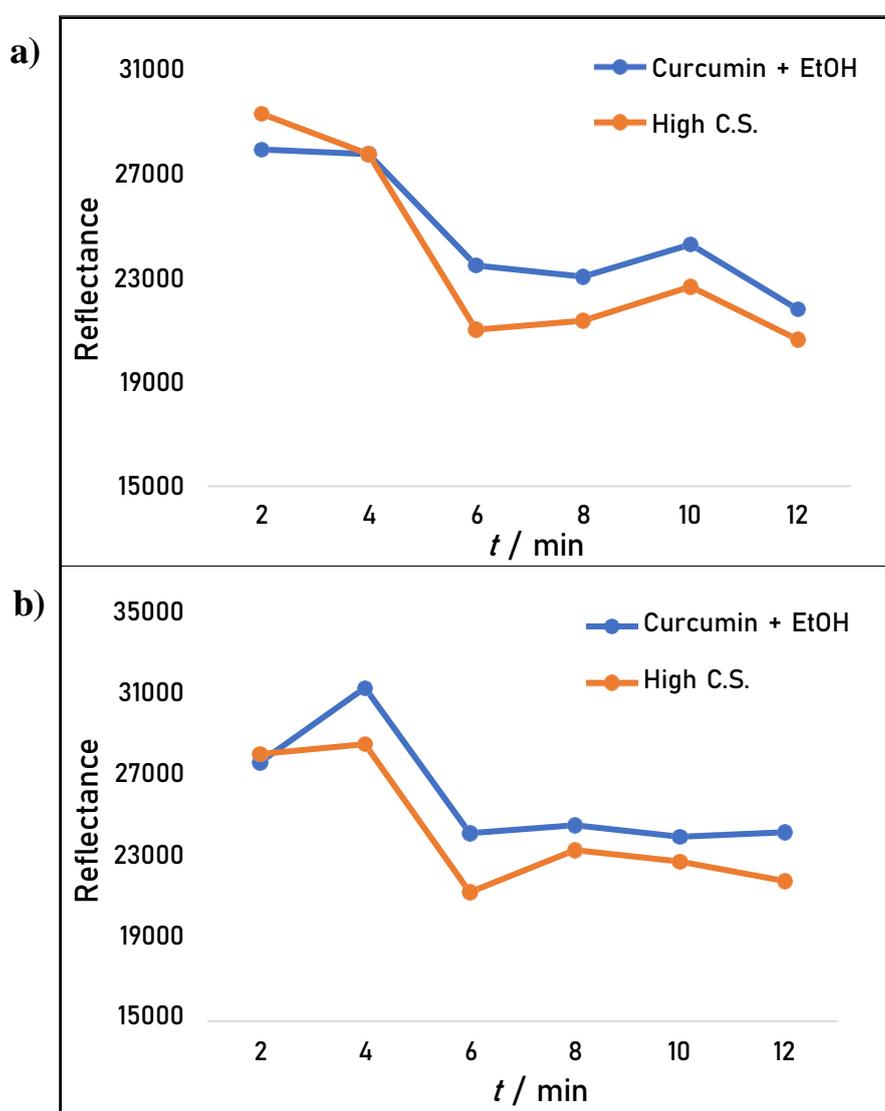
Figure 24. Stability test results at 640 nm for Curcumin + EtOH (blue line) and High C.S. paper strip (orange line) at: a) pH = 6, and b) pH = 8.
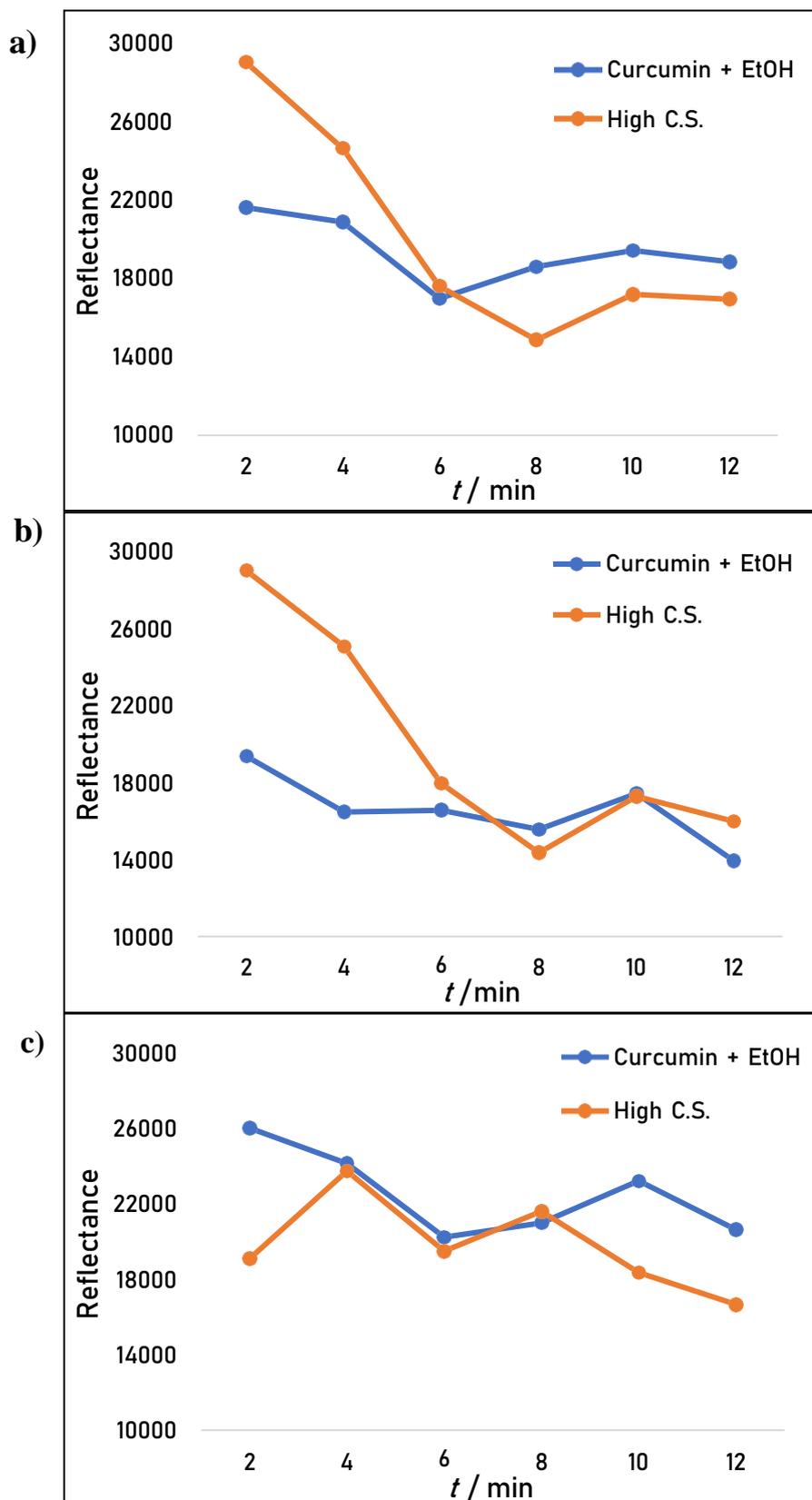
Figure 25. Stability test results at 640 nm for Curcumin + EtOH (blue line) and High C.S. paper strip (orange line) at: a) pH = 10, b) pH = 12, and c) pH =13.

At pH 6 and 8, behavior of curcumin-based paper sensor is very similar for both curcumin in EtOH and in sol with the highest intensity decrease at $t_3 = 6$ min, after which no significant changes were noticed (Fig. 12). At higher pH, 10 and 12, a large difference in initial intensities can be noticed, where curcumin in sol has higher reflectance intensity and steeper fall with time (Figure 25.) This can be attributed to curcumin encapsulation in silica network, because of which it takes longer for the buffer solution to penetrate to the curcumin, which can be attained by visual inspections as well (Figure 26). On the other hand, curcumin paper sensors without silica network support are more prone to leaching at pH 10 and 12, which is why their reflectance intensity is significantly lower in the first 4 minutes, compared to High C.S. paper strips.
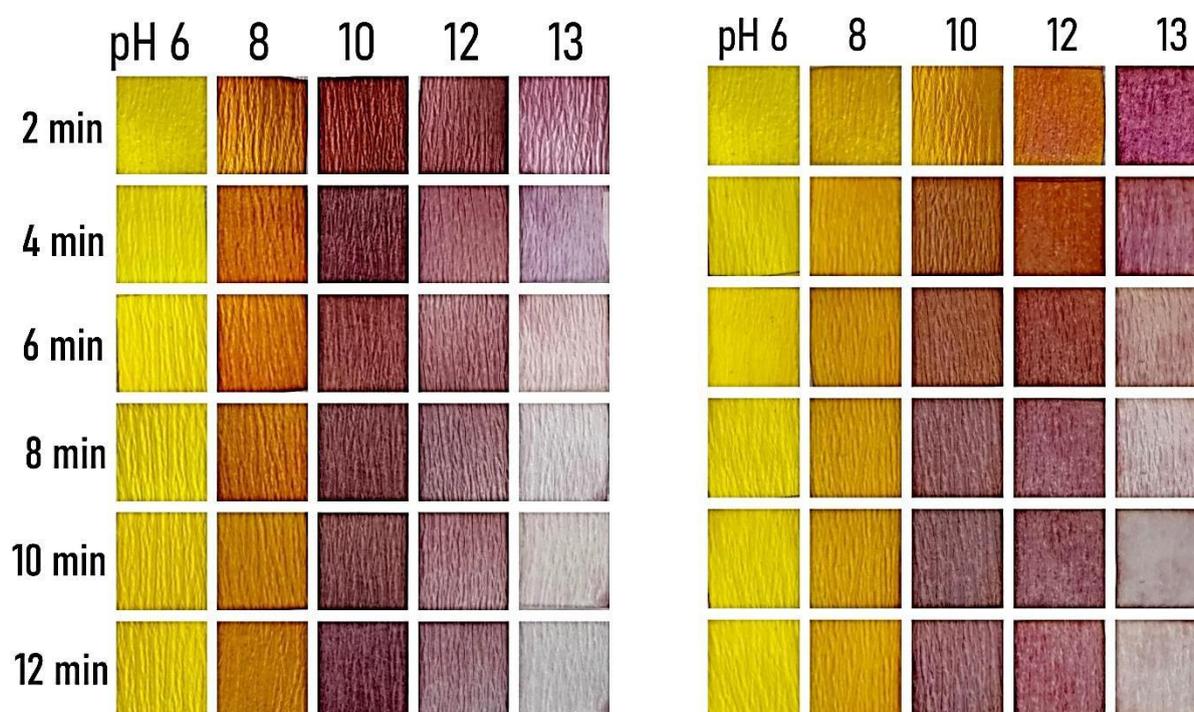
Figure 26. Visual representation of stability testing for Curcumin + EtOH (left) and High C.S. (right) paper strip at pH = 6 – 13, done in 6 intervals, for 12 min overall.

Few other research already demonstrated that stability of curcumin depends on pH, the carrier type and functionalization [34,53,54]. Jain et al. discovered that stability of curcumin formulated with organically modified silica nanoparticle (NP) carrier functionalized with

3-amino propyl group was significantly high, but still much lower than in case of curcumin immobilized in serum protein and liposome, but in all cases, stability of curcumin decreased with the increase in pH from 5 to 8.5 [53]. Dias et al. also concluded that curcumin shows different stability regarding the pH of the environment, discovering that in acidic to neutral solution (pH = 3 – 7), the half-life of curcumin is around 200 min, whereas in basic solution (pH > 7), the half-life is around 10 min [34]. Furthermore, few other studies demonstrated that in a phosphate buffer at pH 7.2, more than 90% of curcumin degrades after 30 minutes, while in the pH range of 1.2 to 6, the degradation is less than 10%. [53,54]. According to all literature, the enhanced stability of curcumin at acidic pH is attributed to the conjugated diene structure, which at neutral or basic pH is disrupted by the loss of the proton from the phenolic group, turning curcumin into anionic form [34,53,54].

4.2.7. Reversibility Performance

Reversibility testing was done in 5 cycles according to previously described procedure (3.7.). The highest change in reflectance intensity between immersion in buffer solution of pH 6 and 10 occurred at 540 nm, so aforementioned wavelength was chosen for graph plotting of reversibility of Curcumin + EtOH and High C.S. paper strip, and the results are represented in Figure 27.
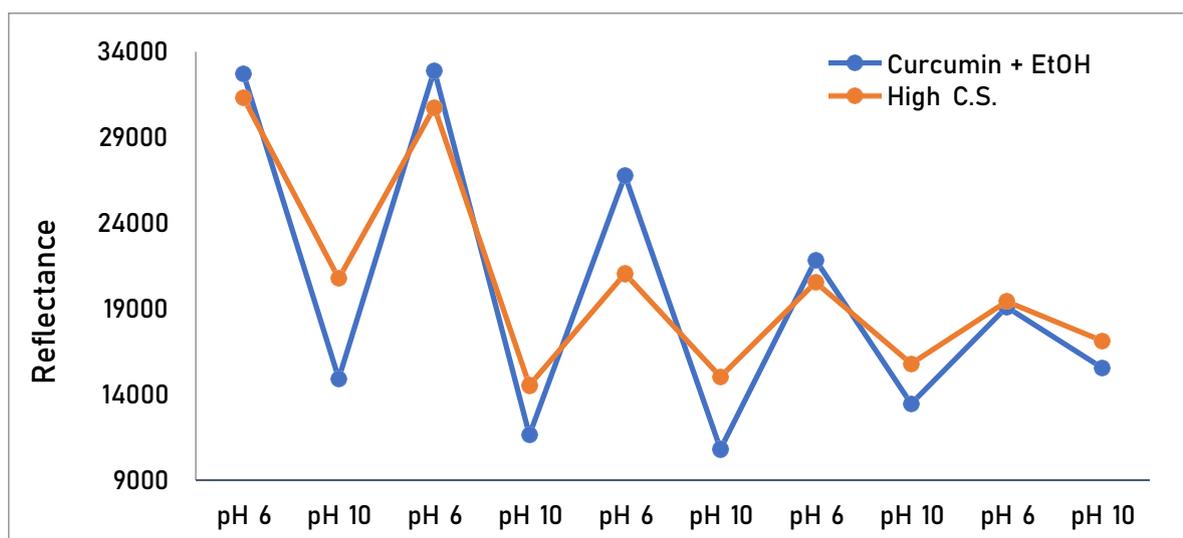
Figure 27. Reversibility test results at 540 nm for Curcumin + EtOH (blue line) and High C.S. paper strips (orange line) at pH = 6 and 10, interchangeably.

Both paper strips showed good reversibility for first 4 measurements, first 2 cycles, (Fig 27.) after which the peak of reflectance intensity strongly lowered because curcumin dye started to leach out. At the same time, the difference between the peaks at pH 6 and 10 also started to decrease after 2nd cycle, and stopped recovering to initial reflectance intensities. Relative changes of intensity were calculated for both paper strips in relation to the first measured intensity of reflectance at pH = 6 and pH = 10, and are presented in Table 9.

Table 9. Calculated relative change of intensity of Curcumin + EtOH and High C.S. paper strips.

Curcumin + EtOH ($c = 1.0 \times 10^{-3}$ M) paper strips							
	pH 6				pH 10		
Intensity change / %	0.56	18.25	33.25	41.66	22.06	27.62	9.82	4.25
High C.S. ($c = 1.0 \times 10^{-3}$ M) paper strips							
Intensity change / %	1.77	32.78	34.40	37.97	30.02	27.62	23.91	17.52

For Curcumin + EtOH paper strip, the reflectance intensity firstly rose for 0.56 % at pH 6, after which it started to fall, and finally fell to 41.66 % of the initial value, while at pH 10 it was constantly getting lower, with the highest difference of 22.06 % at the beginning, which was lowering with each measurement, and finally reaching 4.25 %. Almost identical behavior was observed for High C.S. paper strips, where intensity of reflectance at 6 pH was dropping from the start compared to initial value, with a small difference of 1.77% at first, which increased to 37.97 % after the 5th cycle. At pH 10, the same pattern as in Curcumin + EtOH paper strip was observed again, with the highest intensity difference of 30.02 % after the 1st cycle, which was getting lower as curcumin dye was leaching out, falling to 17.52 % at the end.

Furthermore, Curcumin + EtOH – based paper sensor showed very intense color change between pH 8 and 10, as shown in Figure 28., while High C.S. paper strip required longer exposure to buffer solution in order to achieve visible color change. This is most likely due to reduced accessibility of curcumin when encapsulated in silica network. Nevertheless, both curcumin-based paper sensors showed acceptable color change for naked eye detection of pH between 6 and 10, and therefore both could be used for optical sensing up to 5 cycles until the curcumin dye considerably start to leach out.
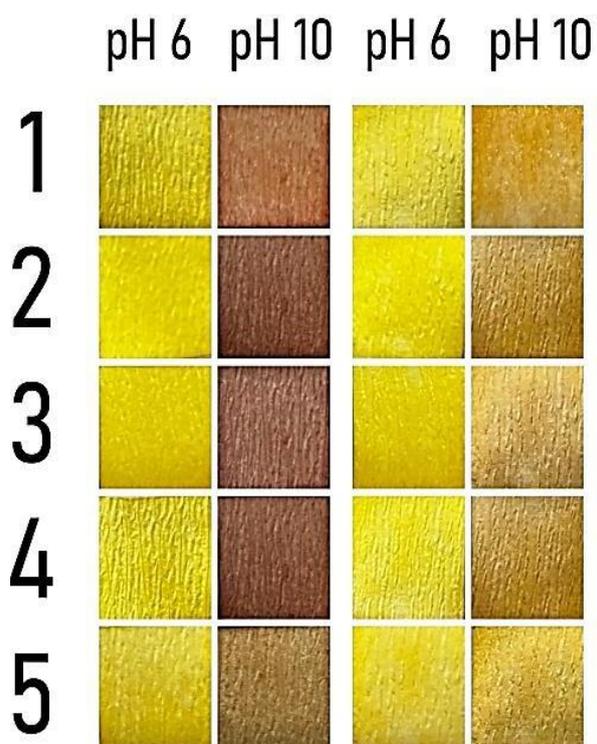
Fig 28. Paper strips of Curcumin + EtOH (left) and High C.S. (right) after immersion in buffer solutions of pH 6 and 10 and drying; repeated for 5 cycles.

5. CONCLUSION

Analytical platforms for rapid sensing using curcumin-immobilized by sol-gel method and implemented on two different substrate materials: glass and paper, were successfully developed, and the possibility of their application as optical sensors was investigated. The curcumin-based glass and paper sensor performance was assessed using buffer solutions in the pH range 4 – 13. Through a careful examination of the behavior of the sensory components on a particular substrate, it was determined that the paper is the best of the tested substrate materials, and the selection was supported by the results of spectroscopic characterization.

By examining different parameters of the characterization of curcumin-based paper sensor in comparison to curcumin and EtOH solution, the following was established:

- ➢ Curcumin concentration of $c = 1.0 \times 10^{-3}$ M is applicable for immobilization and application in optical sensors for naked-eye colorimetric detection.
- ➢ The keto form of curcumin is responsible for the yellowish hue of paper sensor in acidic and neutral media, but at higher pH bathochromic shift occurs due to predominance of enol form in alkaline media which gives the paper sensor its red and brownish-orange hue.
- ➢ The isosbestic point at $\lambda = 525$ nm denotes a balance between the dianionic form at pH = 10.0 – 11.0 and the completely deprotonated form at pH = 12.0, resulting in a red solution in basic media. This is because curcumin has three acidic hydrogens (from one enolic and two phenolic groups), which, according to its enol form structure, can dissociate.
- ➢ Both paper strips, with and without immobilization of curcumin in silica sol-gel matrix, showed a maximum reflectance at 650 nm from pH = 9.03 to 13.20 which can be attributed to deprotonated form of curcumin dye, while the protonated form had a maximum reflectance at 574 nm for all pH levels up to 7.47.
- ➢ When curcumin is immobilized by sol-gel (High C.S. paper strip), it exhibits the greatest color shift between pH 10.0 and 13.0., but when not immobilized (Curcumin + EtOH paper strip), the greatest intensity rise occurs at lower pH values, between 8.5 and 10.0, which can be attributed to curcumin being trapped in the silica network.

- Entrapment of curcumin in silica network creates a barrier for the buffer solution making it more difficult for it to reach the curcumin dye, but it also prevents leaching out of curcumin and enhances performance of the sensing material.

- Stability of curcumin immobilization depends on the pH, the carrier type and functionalization. The conjugated diene structure, which is disturbed at neutral or basic pH by the loss of the proton from the phenolic group and converts curcumin into anionic form, is responsible for curcumin's increased stability at acidic pH.

- Curcumin-based paper sensors could be utilized for optical sensing for a short period of time, before the curcumin dye starts to leach out. Further optimization may be needed for specific applications.

In conclusion, paper-based strips combined with natural indicator dyes have a great potential as chemical sensor and biosensor materials because they may offer simple instantaneous detection of analytes by naked eye, thus avoiding use of complex and expensive instrumentation. Thus, fabrication methods using "green" deposition techniques that use non-toxic reagents, water as a solvent, and manufacturing techniques that limit the exposure of the operators to toxic aerosols will be the biggest challenge in the coming years. When creating new materials for the future, the environment must be given top consideration.

6. BIBLIOGRAPHY

[1] MacCraith, B. D., McDonagh, C. M., O'Keeffe, G., McEvoy, A. K., Butler, & T., Sheridan, F. R. (1995). Sol-gel coatings for optical chemical sensors and biosensors. *Sensors and Actuators B: Chemical*, 29(1), 51-57. doi:10.1016/0925-4005(95)01662-7

[2] Khorasani, M. Y., Langari, H., Sany, S. B. T., Rezayi, M., & Sahebkar, A. (2019). The role of curcumin and its derivatives in sensory applications. *Materials Science and Engineering: C*, 103, 109792. doi:10.1016/j.msec.2019.109792

[3] Wulandari, A., Sunarti, T., Fahma F., & Enomae, T. (2020). The potential of bioactives as biosensors for detection of pH. *IOP Conf. Series: Earth and Environmental Science,* 460

[4] Arafa, A. A., Nada, A. A., Ibrahim, A. Y., Zahran, M. K., & Hakeim, O. A. (2021). Greener therapeutic pH-sensing wound dressing based on Curcuma Longa and cellulose hydrogel. *European Polymer Journal*, 159, 110744. doi:10.1016/j.eurpolymj.2021.110744

[5] Wencel, D., Abel, T., & McDonagh, C. (2014). Optical Chemical pH Sensors. *Analytical Chemistry*, 86(1), 15-29. doi:10.1021/ac4035168

[6] Mahboubeh, V., Rounaghi, G. H., Es'haghi, Z., & Moradi, Z. (2019). Design and Application of an Optical pH Sensor Based on Thionine Doped Modified Sol–Gel Film. *Russian Journal of Physical Chemistry A*, 93(7), 1389-1393. doi:10.1134/S0036024419070173

[7] Zhang, J., & Zhou, L. (2018). Preparation and Optimization of Optical pH Sensor Based on Sol-Gel. Sensors (Basel, Switzerland), 18(10), 3195. doi:10.3390/s18103195

[8] Safavi, A., & Bagheri, M. (2003). Novel optical pH sensor for high and low pH values. *Sensors and Actuators B: Chemical*, 90, 143-150. doi:10.1016/S0925-4005(03)00039-X

[9] Chapter 2 History of Chemical Sensing. 5-18. https://labs.ece.uw.edu/denise/www/Lab/publications/PhD/chapter2.pdf (Accessed May 13 2022)

[10] Shakeri, A., Jarad, A. N., Leung, A., Soleymani, L., & Didar, T. (2019). Biofunctionalization of Glass- and Paper-Based Microfluidic Devices: A Review. *Advanced Materials Interfaces*, 6, doi:10.1002/admi.201900940

[11] Tang, T., Yuan, Y., Yalikun, Y., Hosokawa, Y., Li, M., & Tanaka, Y. (2021). Glass based Micro Total Analysis Systems: Materials, Fabrication methods, and Applications. *Sensors and Actuators: B. Chemical*. doi:10.1016/j.snb.2021.129859

[12] Qi, Z.B., Xu, Li., Xu, Y., Zhong, J., Abedini, A., Chenga, X., & Sinton, D. (2018). Disposable silicon-glass microfluidic devices: precise, robust and cheap. *Lab Chip*, 18, 3872.

[13] Nishat, S., Turab Jafry, A., Martinez, A.W., & Rabbi Awan, F. (2021). Paper-based microfluidics: Simplified fabrication and assay methods. *Sensors & Actuators: B. Chemical*, 336, 129681.

[14] Noviana, E., Ozer, T., Carrell, C.S., Link, J.S., McMahon, C., Jang, I., & Henry, C.S. (2021). Microfluidic Paper-Based Analytical Devices: From Design to Applications. *Chemical Reviews*, 121(19), 11835-11885.

[15] Abdollahi-Aghdam, A., Majidi, M.R., & Omidi, Y. (2018). Microfluidic paper-based analytical devices (µPADs) for fast and ultrasensitive sensing of biomarkers and monitoring of diseases. *BioImpacts*, 8(4), 237-240.

[16] Aguilar, G. (2018). Introductory Chapter: A Brief Semblance of the Sol-Gel Method in Research. In. doi:10.5772/intechopen.82487

[17] Brinker, C. J., & Scherer, G. W. (1990). CHAPTER 3 - Hydrolysis and Condensation II: Silicates. In C. J. Brinker & G. W. Scherer (Eds.), Sol-Gel Science (pp. 96-233). Academic Press. Doi:10.1016/B978-0-08-057103-4.50008-8

[18] Dansby-Sparks, R. N., Ouyang, R., & Xue, Z.-L. (2009). Optical and electrochemical sol-gel sensors for inorganic species. Science in China Series B: Chemistry, 52(11), 1777. doi:10.1007/s11426-009-0278-6

[19] Trindade, F., & Politi, M. (2019). Sol-Gel Chemistry—Deals With Sol–Gel Processes. In book: *Nano Design for Smart Gels*, 15-34. doi:10.1016/B978-0-12-814825-9.00002-3

[20] Poddighe, M., & Innocenzi, P. (2021). Hydrophobic Thin Films from Sol–Gel Processing: A Critical Review. *Materials*, 14, 6799. doi:10.3390/ma14226799

[21] Jurmanović, S., Kordić, Š., Steinberg, M. D., & Steinberg, I. M. (2010). Organically modified silicate thin films doped with colourimetric pH indicators methyl red and bromocresol green as pH responsive sol–gel hybrid materials. *Thin Solid Films*, 518(8), 2234-2240. doi:10.1016/j.tsf.2009.07.158

[22] Tripathi, V. S., Kandimalla, V. B., & Ju, H. (2006). Preparation of ormosil and its applications in the immobilizing biomolecules. *Sensors and Actuators B: Chemical*, 114(2), 1071-1082. doi:10.1016/j.snb.2005.07.037

[23] Kassal, P., Šurina, R., Vrsaljko, D., & Steinberg, I. M. (2014). Hybrid sol–gel thin films doped with a pH indicator: effect of organic modification on optical pH response and film surface hydrophilicity. *Journal of Sol-Gel Science and Technology*, 69, 586-595.

[24] Cui, Z., & Liao, L. (2020). 6 - Coating and printing processes. In book: *Solution Processed Metal Oxide Thin Films for Electronic Applications*, 83-97. doi:10.1016/B978-0-12-814930-0.00006-2

[25] Yilbas, B. S., Al-Sharafi, A., & Ali, H. (2019). Chapter 3 - Surfaces for Self-Cleaning. In book: *Self-Cleaning of Surfaces and Water Droplet Mobility*, 45-98. doi:10.1016/B978-0-12-814776-4.00003-3

[26] Boudrioua, A., Chakaroun, M., & Fischer, A. (2017). 2 - Organic Light-emitting Diodes. In book: *Organic Lasers*, 49-93. doi:10.1016/B978-1-78548-158-1.50002-X

[27] Gründler, P. (2007). Optical Phenomena and Spectroscopy. In book: *Chemical Sensors. An Introduction for Scientists and Engineers*, 27-34.

[28] Munjanja, B., & Sanganyado, E. (2015). UV–Visible Absorption, Fluorescence, and Chemiluminescence Spectroscopy. In book: *Handbook of Food Analysis*, 3(31), 572-583.

[29] Hulanicki, A., Glab, S., & Ingman, F. (1991). Chemical Sensors Definitions and Classification. *Pure Appl. Chem.*, 63, 1247-1250.

[30] Expii. (Accessed July 4, 2022). Color and Oxidation State — Overview & Examples. https://www.expii.com/t/color-and-oxidation-state-overview-examples-8411

[31] Schaepman-Strub, G., Schaepman, M.E., Painter, T.H., Dangel, S., & Martonchik, J.V. (2006). Reflectance Quantities in Optical Remote Sensing – Definitions and Case Studies. *Remote Sens. Environ.,* 103, 27-42.

[32] Narayanaswamy, R. (1993). Optical Chemical Sensors: Transduction and Signal Processing. *Analyst*, 118, 317-322.

[33] Džimbeg-Malčić, V., Barbarić-Mikočević, Ž., & Itrić, K. (2011). Kubelka-Munk Theory in Describing Optical Properties of Paper. *Technical Gazette*, 18 117-124.

[34] Dias, L.D., Blanco, K.C., Mfouo-Tynga, I.S., Inada, N.M., & Bagnato, V.S. (2020). Curcumin as a photosensitizer: From molecular structure to recent advances in antimicrobial photodynamic therapy. *Journal of Photochemistry and Photobiology C: Photochemistry Reviews*, 45, 100384.

[35] Boruah, B., Saikia, P.M., & Dutta, R.K. (2012). Binding and stabilization of curcumin by mixed chitosan–surfactant systems: A spectroscopic study. *Journal of Photochemistry and Photobiology A: Chemistry*, 245, 18– 27.

[36] Xu, G., Wang, J., Si, G., Wang, M., Xue, X., Wu, B., & Zhou, S. (2016). A novel highly selective chemosensor based on curcumin for detection of Cu^{2+} and its application for bioimaging. *Sensors and Actuators B: Chemical*. doi:10.1016/j.snb.2016.02.110

[37] Priyadarsini, K.I. (2014). The Chemistry of Curcumin: From Extraction to Therapeutic Agent. *Molecules*, 19, 20091-20112. doi:10.3390/molecules191220091

[38] Nardo, L., Andreoni, A., Masson, M., Haukvik, T., & Tønnesen, H.H. (2011). Studies on Curcumin and Curcuminoids. XXXIX. Photophysical Properties of Bisdemethoxycurcumin. *J Fluoresc.*, 21, 627–635.

[39] Moussawi, R.N., & Digambara Patra, D. (2016). Modification of nanostructured ZnO surfaces with curcumin: fluorescence-based sensing for arsenic and improving arsenic removal by ZnO. *RSC Adv.*, 6, 17256.

[40] Wang, Y.J., Pan, M.H., Cheng, A.L., Lin, L.I., Ho, Y.S., Hseieh, C.Y., & Lin, J.K. (1997). Stability of curcumin in buffer solutions and characterization of its degradation products. *J. Pharm. Biomed. Anal.*, 15, 1867–1876.

[41] Semalty A, Semalty M, Rawat M.S.M, & Franceschi F. (2010). Supramolecular phospholipids-polyphenolics interactions: The PHYTOSOME (R) strategy to improve the bioavailability of phytochemicals. *Fitoterapia*, 81, 306–314. doi:10.1016/j.fitote.2009.11.001

[42] Shah, C.P., Mishra, B., Kumar, M., Priyadarsini, K.I., & Bajaj, P.N. (2008). Binding studies of curcumin to polyvinyl alcohol/polyvinyl alcohol hydrogel and its delivery to liposomes. *Current Science*, 95, 1426–1432.

[43] Takahashi, M., Uechi, S., Takara, K., Asikin, Y., & K. Wada (2009). Evaluation of an oral carrier system in rats: bioavailability and antioxidant properties of liposome encapsulated curcumin. *Journal of Agricultural and Food Chemistry,* 57, 9141–9146.

[44] Kaminaga, Y., Nagatsu, A., Akiyama, T., Sugimoto, N., Yamazaki, T., Maitani, T., & Mizukami, T. (2003). Production of unnatural glucosides of curcumin with drastically enhanced water solubility by cell suspension cultures of Catharanthus roseus. *FEBS Letters*, 555, 311–316.

[45] Barik, A., Priyadarsini, K.I., & Mohan, H. (2003). Photophysical studies on binding of curcumin to bovine serum albumin. *Photochemistry and Photobiology*, 77, 597–603.

[46] Kim, C.Y., Bordenave, N., Ferruzzi, M.G., Safavy, A., & Kim, K.-H. (2011). Modification of curcumin with polyethylene glycol enhances the delivery of curcumin in preadipocytes and its antiadipogenic property. *Journal of Agricultural and Food Chemistry*, 59, 1012–1019.

[47] Lee, W.-H., Loo, C.-Y., Bebawy, M., Luk, F., Mason, R.S., & Rohanizadeh, R. (2013). Curcumin and its Derivatives: Their Application in Neuropharmacology and Neuroscience in the 21st Century.*Curr Neuropharmacol*, 11(4), 338–378. doi:10.2174/1570159X11311040002

[48] Martínez-Guerra, J., Palomar-Pardavé, M., Romero-Romo, M., Corona-Avendaño, S., Rojas-Hernández, A., & Ramírez-Silva, M.T. (2019). New insights on the Chemical Stability of Curcumin in Aqueous Media at Different pH: Influence of the Experimental Conditions. *Int. J. Electrochem. Sci*., 14, 5373 – 5385, doi:10.20964/2019.06.24

[49] Subhan, M.A., Alam, K., Rahaman, M.S., & Atiqur Rahman, M. (2014). Synthesis and Characterization of Metal Complexes Containing Curcumin ($C_{21}H_{20}O_6$) and Study of their Anti-microbial Activities and DNA Binding Properties. *Journal of Scientific Research*, 6(1), 97-109. doi:10.3329/jsr.v6i1.15381

[50] Bernabé-Pineda, M., Ramirez-Silva, M.T., Romero-Romo, M., González-Vergara, E., & Rojas-Hernández, A. (2004). Determination of acidity constants of curcumin in aqueous solution and apparent rate constant of its decomposition. *Spectrochimica Acta Part A*, 60(5), 1091–1097.

[51] Anjomshoa, S., Namazian, M., & Noorbala, M.R. (2016). The Effect of Solvent on Tautomerism, Acidity and Radical Stability of Curcumin and Its Derivatives Based on Thermodynamic Quantities. *J Solution Chem*, 45, 1021–1030. doi:10.1007/s10953-016-0481-y

[52] Zhao, Q., Kong, D.-X., & Zhang, H.-Y. (2008). Excited-State pK_a Values of Curcumin. *Natural Product Communications*, 3(2), 229-232. doi:10.1177/1934578X0800300225

[53] Jain, B. (2016). A spectroscopic study on stability of curcumin as a function of pH in silica nanoformulations, liposome and serum protein, *Journal of Molecular Structure*. doi:10.1016/j.molstruc.2016.10.014.

[54] Zaghary, W.A., Hanna, E.T., Zanoun, M.A., Abdallah, N.A., & Sakr, T.M. (2019). Curcumin: Analysis and Stability. *J. Adv. Pharm. Res.,* 3(2), 47-58. doi:10.21608/APRH.2019.6191.1069

7. CURRICULUM VITAE

Marija Šiprak ████████████████████████████████████ After successfully passing the state exam and finishing Grammar School in Bjelovar, in 2016 she enrolled in an undergraduate course of Applied Chemistry at the Faculty of Chemical Engineering and Technology (FCET), University of Zagreb. As part of the teaching curriculum, she did a professional internship in Pliva (Teva) in 2019. In the same year, she defended the final thesis entitled *Application of high-throughput glycomics in the research of new biomarkers of diseases and aging*, which was done under the mentorship of Marina Martinić Kavur, PhD, at Genos, Zagreb, and graduated *cum laude*. During her undergraduate studies, she actively participated in *Student's Section of the Croatian Society of Chemical Engineers (CSCE)*, and was a two-time recipient of STEM scholarship for excellence (2017-2019). After finishing Applied Chemistry, she continued her studies at the same Faculty, and in 2019 got enrolled into a new graduate program taught exclusively in Englich, entitled Chemical and Environmental Technology (CET). During this time, she was selected for the *Student's Council of FCET* and was a Student Representative for the course of Applied Chemistry. Furthermore, in 2021 she went on a four-month research internship in Spain through the Erasmus+ program, and studied TiO_2-based photocatalysis for the removal of micro-pollutant pesticides by solar-assisted-photocatalytic processes at the Institute of Catalysis and Petrochemistry, CSIC, Madrid. In 2022, she went on a 1-semester bilateral exchange to the US, studying Food, Nutrition, and Wellness Studies, and Spanish at Indiana University of Pennsylvania (IUP). She finished the exchange with the highest score and was awarded with the Dean's List Certificate of Academic Achievement in recognition of Excellence.